DIPLOMARBEIT

Titel der Diplomarbeit

Neurotrophic Dependency of Sensory Neurons in a Co-Culture Model of Porcine DRGs and Human Skin Cells

angestrebter akademischer Grad

Magister/Magistra der Naturwissenschaften (Mag. rer.nat.)

Verfasserin:	Susanne Martina Falkner
Matrikel-Nummer:	0304600
Studienrichtung (lt. Studienblatt):	A490
Betreuer:	Ao. Prof. Dr. Sigismund Huck

Wien, Juni 2009

The thesis was performed at

Beiersdorf AG, Hamburg
Skin Research Department
Group of Dr. Gitta Neufang

in cooperation with

The Faculty of Clinical Medicine, Mannheim
University Heidelberg
Group of Prof. Dr. Martin Schmelz

Acknowledgements

Table of Content

1   Introduction

1.1   The cutaneous peripheral sensory nervous system

Anatomically, the human nervous system is divided into the central nervous system, CNS and the peripheral nervous system, PNS. While the CNS comprises the brain and the spinal cord, the PNS consists of the efferent postganglionic and the sensory afferent structures of the somatic and autonomic nervous system, including the twelve cranial nerves.

In terms of physiological function, the nervous system is divided into the somatic nervous system of conscious control and the autonomic nervous system, ANS of involuntarily regulated, visceral functions. Both systems consist of afferent sensory neurons and efferent motor neurons, as well as connecting interneurons. The sensory, motor and interneurons of the autonomic nervous system in turn, are arranged in two functional systems: The sympathetic and the parasympathetic autonomic nervous system.

The *peripheral sensory nervous system* therefore includes: The sensory afferents of the somatic nervous system and the sensory sympathetic and parasympathetic afferents of the autonomic nervous system, also called visceral sensory neurons. All of them innervate to varying extent the human skin [1] [2].

1.1.1   Anatomy of the cutaneous peripheral sensory nervous system

The cell bodies of somatic and visceral afferent sensory neurons are located in the dorsal root ganglia, DRG and in the ganglia of the cranial nerves. All sensory neurons are considered pseudounipolar, with the exception of several cranial nerves which contain bipolar neurons [3]. Pseudounipolar neurons possess one bifurcated axon, the long distal process innervating the peripheral target tissue and the short proximal process projecting to the spinal cord. The sensory roots leaving the ganglia converge with the motor roots originating in the brain stem and the spinal cord and form mixed cranial nerves and the 31 pairs of spinal nerves. They branch and proceed in mixed bundles to their peripheral target tissues.

Cutaneous nerves enter the skin via the subcutis which is mainly built of connective and adipose tissue. Nerve bundles proceed to the subsequent dermis, which primarily consists of fibroblasts that secrete the main components of the extracellular matrix, in particular the glycoproteins elastin, fibronectin and collagen [4]. The dermis further

contains microvascular blood and lymphatic vessels, as well as the skin appendages and immune cells [5] [6]. In the dermis nerve bundles loosen and axonal fibers branch to build the dermal nerve plexi. Autonomic motor and sensory fibers, mainly of the sympathetic and to minor extent of the parasympathetic system, innervate the arteriovenous anastomoses, the microvascular blood and lymphatic vessels, the sebaceous and sweat glands and the hair follicles with the erector pili muscles [7]. However, autonomic fibers do not enter the superficial epidermal layer of the skin. In contrast, the somatic sensory neurons either terminate in the dermis or in the epidermis. In the dermis somatic sensory neurons end as encapsulated mechanoreceptors (Pacinian, Meissner and Ruffini corpuscles), innervate the hair follicles or form free sensory nerve endings [8]. In the epidermis the somatic sensory neurons generally terminate as free nerve endings or in complex with Merkel cells located in the epidermal basal layer [9]. The predominant cell type of the epidermis constitute keratinocytes with up to 85 to 95 percent, followed by melanocytes, Langerhans cells and Merkel cells. Keratinocytes undergo terminal differentiation, a mechanism of controlled cell death that results in denucleated, cornified cells of the horny layer [10] [11]. Keratinocytes of different stages of differentiation form the characteristic squamous stratified epithel which is subclassified into the 5 epidermal layers: *stratum basale* , *stratum spinosum*, *stratum granulosum*, *stratum lucidum* and *stratum corneum* **(Figure 1)**.

Unmyelinated somatic sensory fibers branch extensively at the dermal-epidermal borders and create a three dimensional network of sensory fibers throughout the epidermis [12] [13]. The most superficial fibers reach into the *stratum granulosum*. Different sensory fiber types terminate in distinct keratinocyte layers and may serve different functional purpose, as indicated by Zylka MJ. in 2005 [14].
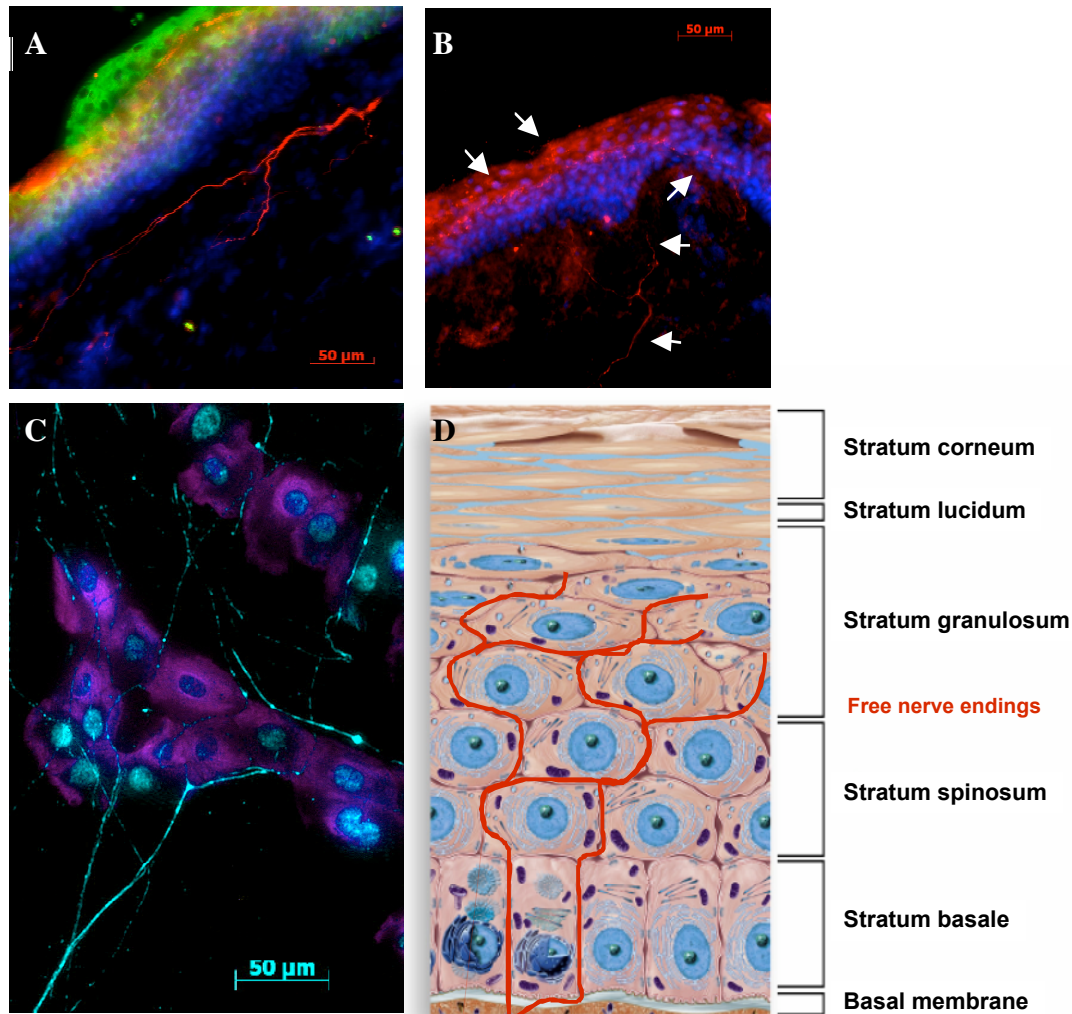
Figure 1: Topography of nerve fibers in the skin
A) Human dermal nerve plexus and **B)** neuronal fibers entering the epidermis (arrows); Cryosections of human punch biopsies, neurites labeled with mouse monoclonal anti-SMI312 and goat anti-mouse Alexa 594, keratinocytes labeled with rabbit polyclonal anti-cytokeratin 1/10 and goat anti-rabbit Alexa 488, nuclei labeled with DAPI (Zeiss Axiovert S100; 100x magnification)
C) *In-vitro* co-culture of sensory neurites and primary human keratinocytes; Keratinocytes labeled with rabbit polyclonal anti-wide spectrum cytokeratin and goat anti-rabbit Alexa 488, neurites labeled with mouse monoclonal anti-SMI312 and goat anti-mouse Alexa 594 (Zeiss Axiovert S100; 200x magnification)
D) Sketch of the squamous morphology of the human epidermis (modified from Eucerin®)

1.1.2 Classification of sensory neurons

Sensory neurons can be classified into four subgroups according to their extent of myelination and conduction velocity: Aα, Aβ, Aδ and C fibers [15]. In short, Aα fibers possess the largest diameters of 12 – 20 µm at a maximum conduction velocity of 120 m/s, followed by Aβ fibers (6 – 12 µm; max. 70 m/s), Aδ (1 – 5 µm;

max. 30 m/s) and C fibers (0,2 – 1,5 μm; max. 2 m/s). Sensory Aα nerve fibers innervate the proprioceptive organs of muscles, the golgi tendon organ and the muscle spindle [16]. Sensory Aβ fibers form the secondary afferent endings in the muscle spindle and innervate all mechanorecpetive structures in the dermis (1.1.1). Sensory Aδ and C fibers, terminate as free nerve endings in the skin, whereas only C fibers proceed into the epidermal layer **(Figure 2)**. Subtypes of both fiber types respond to temperature and osmotic changes, as well as mechanical, chemical and noxious stimuli [17].
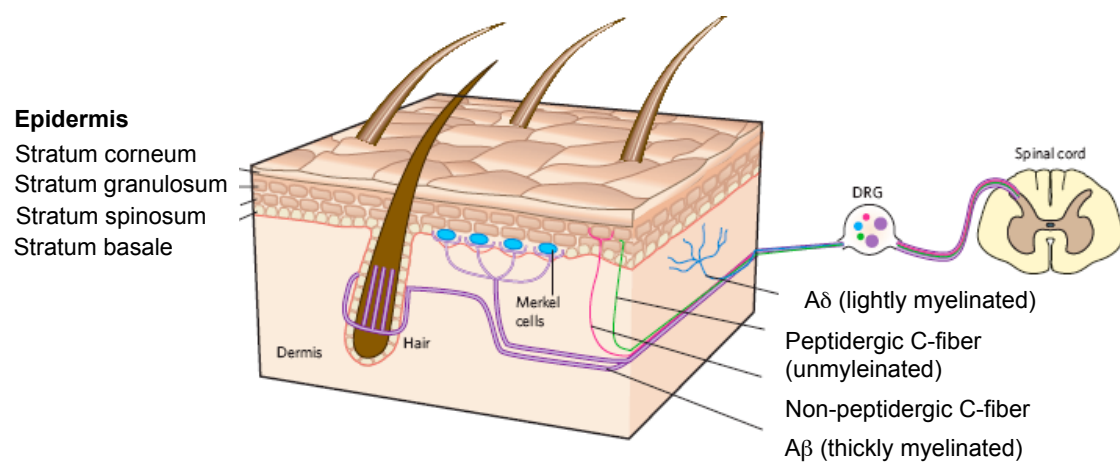
Figure 2: Different classes of somatic sensory fibers innervate the human skin
Somatic sensory fibers derived from DRGs innervate different layers and structures of the skin. Aβ fibers innervate mechanoreceptive skin appendages, Aδ fibers terminate as free nerve endings in the dermis, while unmyelinated C fibers terminate in complex with Merkel cells or as free nerve endings in the epidermis. (modified from Lumpkin&Caterina 2007)

Transient receptor potential channel subfamilies have been implicated as molecular sensors involved in a variety of the above indicated sensations [18]. Warming and cooling sensation is transmitted via TRPV1 – 4 and TRPA1 and M8, respectively. TRPC5 has been implicated in osmosensing [19] and the TRPN and P subfamilies have been related to mechanosensing. In addition, TRPV, TRPA and M subtypes have been detected on nociceptive fibers [20] [21] and several exogenous and endogenous ligands to TRP channels have been identified [22] [23].

Aδ and C nerve fibers that signal pain in response to noxious stimuli are generally termed nociceptors. Different nociceptor subtypes are defined based on the fiber type and conduction velocity, the soma size, the modalities of stimulation and the characteristics of pain sensation transmitted, for instance sharp, pungent or burning [24].

In addition, different types of nociceptive sensory neurons can be subdivided according to their expression of specific molecular markers, including neurofilaments, neuropeptides, enzymes, receptors, as well as their neurotrophic dependency [24]. In rat, approximately 40 % of DRGs stain for NF200, heavy neurofilament 200 kDa, a marker for myelinated neurons. Only 10 % of NF200^{+} neurons are nociceptive, the nociceptive Aδ fibers. NF200^{+} Aδ and NF200^{-} fibers are subclassified into peptidergic and non-peptidergic nociceptors. Peptidergic neurons contain neuropeptides as substance P (SP) or calcitonin gene related peptide (CGRP). They depend on nerve growth factor (NGF) for survival and sustainment of their receptive properties [25]. Accordingly, peptidergic neurons express the NGF high affinity receptor TrkA. Non-peptidergic neurons express the specific surface proteoglycan versican that binds the plant lectin isolectin B4 (IB4) [26] [27]. They are dependent on glial cell-line derived neurotrophic factor (GDNF) and express its receptor tyrosine kinase Ret and the co-receptors GFRα (1-4). TRPV1 is expressed in subpopulations of both, peptidergic and non-peptidergic neurons **(Figure 3)**.

Notably, molecular markers show no specificity for target tissues, considerable overlap exists [28] and marker expression varies substantially between species [29] [28] and developmental stages [30] [31]. Despite these limitations, above indicated markers remain valuable for the general classification of sensory neurons and are combined and extended with different functional properties [32].
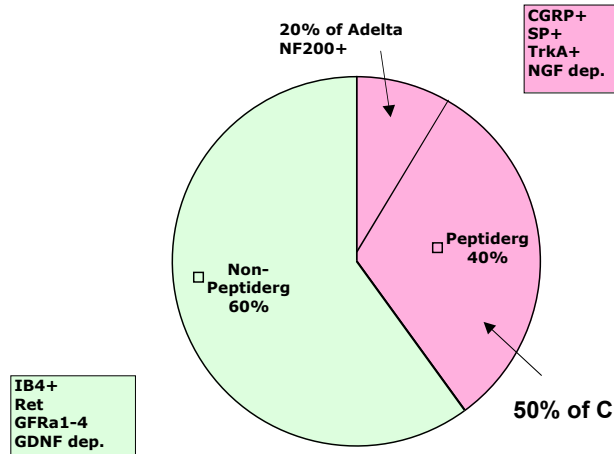
Figure 3: Molecular markers of nociceptive neurons
Nociceptive neurons are divided into peptidergic and non-peptidergic neurons by the expression of molecular markers. Peptidergic: SP$^+$, CGRP$^+$, TrkA$^+$ and dependent on NGF; Non-peptidergic: IB4$^+$, Ret$^+$, GFRα^+ and dependent on GDNF. Note that 20 % of NF200$^+$ Aδ fibers and 50 % of C fibers are peptidergic; Values given for immunofluorescent studies in rats (based on McMahon 2005, Priestly 2002).

1.1.3 Efferent functions of cutaneous sensory neurons

The classical view of sensory nerves in the skin assigns afferent sensory transmission and efferent release of neurotransmitters, neuropeptides and neurohormones to separate anatomical entities. However, present knowledge strongly indicates that sensory reception and efferent release of neuromediators occur at the very same sensory afferent ending. A more and more complex auto and para-neuroendocrine system between nerve fibers, cutaneous cells, immune cells and the microvascular system in the skin becomes apparent **(Figure 4)** [24] [33] [34].

Sensory C and Aδ fibers have been shown to produce and release neuropeptides, as substance P (SP) or calcitonin gene related peptide (CGRP), neurotransmitters as acetylcholine (ACh) and catecholamines (norepinephrine, NE; dopamine) and neurotrophins as NGF. Respective cognate receptors are expressed on numerous cell types in the skin including keratinocytes, fibroblasts, endothelial cells, smooth muscle cells, Merkel cells, mast cells and leukocytes. Further, indicated cell types have been reported to produce and secrete various neuromodulatory factors themselves [35].

Sensory afferents release neuropeptides in response to a wide range of external and internal stimuli, including extreme temperature, low pH, nitric oxide, UV radiation, ATP or other factors released during tissue injury. Neuropeptides bind and act on adjacent cutaneous cells, which in turn secrete more neuropeptides and

neuromodulatory factors. The so created autonomic feedback loops play an important role in skin homeostasis, but also in neurogenic inflammation, pain or pruritus and is misregulated in a number of cutaneous diseases [36] [37] [38].

Stimulus	Representative receptor
NGF	TrkA
Bradykinin	BK_2
Serotonin	$5\text{-}HT_3$
ATP	$P2X_3$
H^+	ASIC3/VR1
Lipids	PGE_2/CB1/VR1
Heat	VR1/VRL-1
Pressure	DEG/ENaC ?
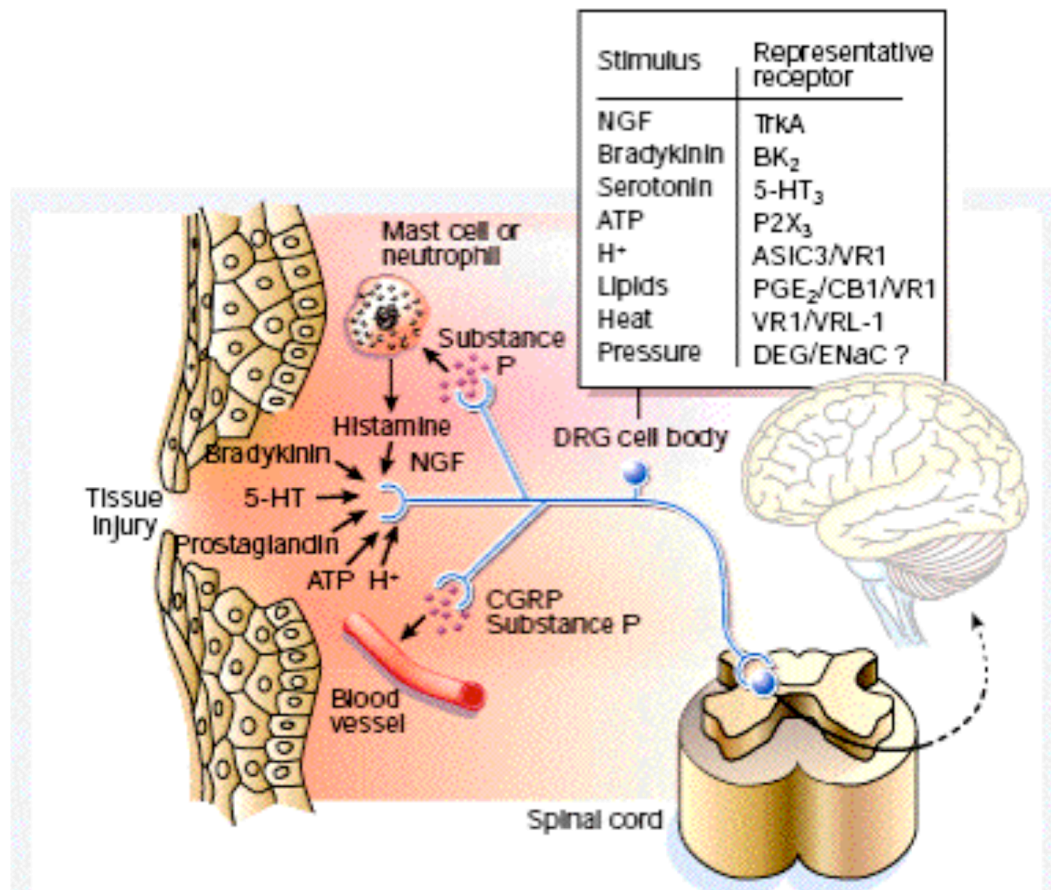
Figure 4: Efferent functions of sensory neurons
Auto and para-neuroendocrine interaction of sensory afferents, skin cells, immune cells and the microvascular system using the example of the neuropeptides SP and CGRP: Acitvated sensory afferents release neuropeptides that activate mast cells and vascular endothelial cells, resulting in the release of cytokines, neurotrophic factors and neuropeptides. (Julius & Basbaum 2001)

1.2   Cutaneous neuropeptides

Neuropeptides are small peptides built of 4 to approximately 40 amino acid residues. Members of the same neuropeptide family are usually transcribed in one large precursor molecule, named pre-pro-neuropeptide. Proteolytic cleavage and posttranslational modifications are required to finally genereate the active neuropeptide. In general, neuropeptides are ligands of G protein coupled receptors (GPCR), thus modulating the excitability of the target cells. Besides the strong expression of neuropeptides and their receptors in the CNS and in the peripheral terminals, they are expressed in nearly all non-neuronal tissues. This allows an extensive crosstalk of neuronal and non-neuronal cells and the integration of different body functions and systems [39].

In the skin, Aδ and C fibers and various cutaneous cell types (1.1.3) have been shown to produce and release neuropeptides including tachykinins (SP, neurokinins NK) [40], VIP/secretin peptides (VIP, PACAP) [41], CGRP peptides [42], opioids and POMC derived peptides [43] [44], as well as endocannabinoids [45]. In summary, they regulate functions in the skin as vasoconstriction and -dilatation and sweat production and -secretion, thus maintaining the skin's temperature and water balance. Neuropeptides possess extensive immune modulatory capabilities. They stimulate the release of pro and anti-inflammatory cytokines, induce the expression of vascular adhesion molecules and exert trophic effects on immune cells, fibroblasts and endothelial cells. Both, cytokines and neuropeptides in turn influence the excitability of sensory afferent nerve endings in the skin [38]. Thus, neuropeptides do not only promote inflammation and wound healing, but play a major role in neuropathic pain and pruritus.

1.2.1   Calcitonin gene related peptide, CGRP

The superfamily of calcitonin gene-related peptides includes CGRP, calcitonin (CT), amylin and adrenomedullin. CGRP1 and CT are encoded in the human CALC I gene, whereas CGRP2 is derived form the CALC II gene. CGRP1 and CGRP2 are built of 37 amino acids and differ in 3 residues. The two subtypes of CGRP1, CGRP1α and CGRP1β, are genereated by alternativ splicing and differ in 1 residue [42] [46]. CGRP1α is the predominant subtype present in sensory neurons, while CGRP1β is found in enteric neurons [47].

Based on affinity and pharmacological studies, two types of receptors have been proposed, CGRP-R1 and CGRP-R2. CGRP-R1 has been identified as a heterodimer of a 7 transmembrane calcitonin-receptor-like receptor (CRLR) and one of three single transmembrane receptor-activity-modifying-proteins, RAMP1. RAMP1 transports CRLR to the plasma membrane. The existence of the CGRP-R2 receptor has recently been questioned as its molecular components remain elusive [48].

In rat skin CGRP is expressed in approximately 51 % of sensory neurons [49] and is found in colocalization with either SP or somatostatin (SST) [50]. CGRP positive fibers are associated with the dermal microvascular system [51]. CGRP was shown to exert potent effects as vasodilator [52] and directly stimulates endothelial cell proliferation, indicating a possible role in angiogenesis and wound healing [53]. CGRP positive fibers are also found closely associated with keratinocytes, melanocytes [54], Merkel cells, Langerhans cells [55] and mast cells [56], which are involved in inflammatory processes. However, some controversy regarding the role of CGRP during inflammation exists. It was shown that CGRP in general exerts an anti-inflammatory effect [57]. On the other hand, it also stimulates neutrophil and monocyte adhesion to microvascular endothelial cells (HDMECs) [58] and the release of pro-inflammatory cytokines, as TNFα, from mast cells [59] [60].

1.3 Cutaneous neurotrophic factors

Per definition, a neurotophic factor exerts trophic, survival and growth effects on neurons. Neurotrophic factors are expressed in the CNS and the peripheral target tissues. They promote and guide innervation during development and ensure the maintainance of neuronal subtypes in the adult organism. The concept of neurotrophic factors was first described by Rita Levi-Montalcini and Stanley Cohen with the discovery of NGF [61].

Subtypes of cutaneous nerve fibers show selective dependency on different neurotrophic factors. They express specific tyrosine kinase receptors that are internalized together with the bound ligand and retrogradely transported to the cell somata, thereby ensuring the survival of the respective neuron [62] [63]. In the skin, neurotrophic factors of the neurotrophin and TGFβ superfamilies are expressed by various cell types including keratinocytes [64] [65], fibroblasts [66], endothelial cells [67] [68] and Merkel cells [69]. Dysregulation of cutaneous neurotrophin levels has

been implicated in several cutaneous diseases, causing pain, hypersensitivity and neuropathic conditions [24] [70].

1.3.1 Nerve growth factor, NGF

Nerve growth factor (NGF) is the most prominent member of the superfamily of neurotrophins that also includes brain derived neurotrophic factor (BDNF), neurotrophin-3 (NT-3) and neurotrophin-4 (NT-4). Mature NGF exists in two forms, a high molecular weight hexameric complex built of $2\alpha : 2\beta : 2\gamma$ subunits named 7S NGF and the βNGF homodimer. 7S NGF is expressed at high levels in murine submaxillary glands, but is absent in most other murine tissue or other species [71]. Accordingly, it was shown that the biological functions of NGF are mediated via its β homodimer [72] [73]. The NGFβ subunit is synthesized as 40 kDa glycosylated proNGF precursor molecule [74]. Pro NGF is released upon neuronal activity and processed to mature NGF of 13 kDa in a plasminogen/ tissue plasminogen activator (tPA) dependent manner in the extracellular space [75].

The NGFβ homodimer binds two classes of receptors, the high affinity receptor TrkA and the low affinity receptor p75. Besides NGF, p75 is bound by all members of the neurotrophin family, as well as the precursor proNGF. While the activation of p75 has been implicated in apoptosis [76], TrkA activation induces signaling to promote the survival and maintenance of the target cell. The phosphorylated receptor-ligand complex is internalized in signaling endosomes that are transported retrograd to the cell somata [77]. Simultaneously, TrkA activates downstream signaling via MAP kinase pathways [78], thereby inducing posttranslational and transcriptional modifications of several ion channels [79].

NGF is essential for the maintenance of the nociceptive phenotype of peptidergic C and Aδ fibers and is a key regulator of nociception in the periphery. It directly influences the sensitivity of nociceptive afferents via sensitization of receptors as TRPV1 [80] or bradykinin receptors [81] and stimulation of TRPV1 expression [82]. Furthermore, the production of neuropeptides such as SP and CGRP is regulated by NGF [83]. Neuropeptides in turn play a key role in inflammation and sensitization of nociceptive afferents (1.2) and mediate the release of pro and anti-inflammatory cytokines (TNFα, IL1α/β, IL6, IL8 and IL10), as well as NGF from skin and immune cells [38] [60] [84].

1.4 The role of peripheral sensory neurons in cutaneous disease

A crucial role for cutaneous sensory neuronal afferents has become apparent in several cutaneous diseases, especially in Atopic Dermatitis (AD) and Psoriasis. Both are chronic inflammatory skin diseases with marked dysregulation in keratinocyte proliferation and differentiation, resulting in skin barrier dysfunction. Plaques of inflamed skin exhibit massive infiltration of immune cells and extensive accumulation of allergen specific IgE [85] [86]. Though, the type of T-cell infiltration presents the main difference between psoriatic and atopic inflamed plaques [87].

Psoriatic and AD skin exhibit increased neuronal fiber density and a marked increase in SP and CGRP positive fibers [88] [89]. As indicated in 1.2 and 1.3 SP and CGRP stimulate the release of cytokines and neurotrophins from cutaneous cell types and immune cells. Accordingly, increased levels of NGF in psoriatic and AD skin have been detected [90]. Cytokines, neuropeptides and NGF in turn cause sensitization of nociceptive afferents and the stimulation of already infiltrated immune cells.

In summary, sensory afferent neurons are not only considerably affected in cutaneous diseases, but account for the sustained and persistent inflammation, pain and pruritus, collectively referred to as neurogenic inflammation.

1.5 Focus of the Diploma Thesis

In this work, the local influence of dermal and epidermal skin cells on sensory afferent nerve growth is investigated using a novel *in-vitro* co-culture system of porcine DRGs and human primary skin cells.

In a first attempt, the co-culture system is established and characterized. The sensitivity of the system in repsonse to the neurotrophic factor human NGFβ is examined. Induced peripheral fibers are classified using common nociceptive markers (1.1.2) and the functionality of cultured neurons is analyzed by stimulating the efferent function of sensory neurons (1.1.3).

Secondly, the effects of primary human keratinocytes and fibroblasts on peripheral sensory fiber growth and morphology is examined. Are skin cells sufficient to induce fiber outgrowth in the co-culture system? Do keratinocytes and fibroblasts exert different effects? Does endogenously produced NGF play a role in skin cell mediated effects and are any other factors beside NGF involved?

Page 22

2 Materials

2.1 Antibodies

Primary Antibodies

Rabbit polyclonal anti-TrkA	Abcam, Cambridge UK
Rabbit polyclonal anti-TRPV1	Abcam, Cambridge UK
Rabbit polyclonal anti-PGP9.5	Abcam, Cambridge UK
Mouse monoclonal anti-CGRP	Abcam, Cambridge UK
Mouse monoclonal anti-Fibroblast Surface Protein	Abcam, Cambridge UK
Rabbit polyclonal anti-wide spectrum Cytokeratin	Abcam, Cambridge UK
Rabbit polyclonal anti-Cytokeratin 1/10	Covance, Emeryville USA
Mouse monoclonal anti-Pan-Axonal Neurofilament	Covance, Emeryville USA
Mouse monoclonal anti-Myelin CNPase	Covance, Emeryville USA
Goat polyclonal anti-NGFβ, affinity purified	R&D, MN USA
Isolectin GS-IB4, Alexa Fluor 488 conjugate	Molecular Probes, OR USA

Secondary Antibodies

Alexa Fluor 488, Goat anti-mouse IgG (H+L)	Molecular Probes, OR USA
Alexa Fluor 488, Donkey anti-goat IgG (H+L)	Molecular Probes, OR USA
Alexa Fluor 488, Goat anti-rabbit IgG (H+L)	Molecular Probes, OR USA
Alexa Fluor 594, Goat anti-mouse IgG (H+L)	Molecular Probes, OR USA
Alexa Fluor 594, Goat anti-rabbit IgG (H+L)	Molecular Probes, OR USA

2.2 Chemicals and Buffers

All solutions were prepared with ultra pure water (ddH$_2$O) using a Milli-Q academic water purification system.

Aceton	Merck, Darmstadt GER
Albumin, Bovine (cohnVfraction >96%)	Sigma-Aldrich, Munich GER
Bayer Baysilone, highly viscous	VWR, Darmstadt GER

Calciumchloride	Merck, Darmstadt GER
Capsaicin	Sigma-Aldrich, Steinheim GER
Capsazepin	A.G.Scientific, San Diego USA
DAPI, dilactate	Sigma-Aldrich, Munich GER
D-Glucose	Merck, Darmstadt GER
Dimethyl sulfoxid (DMSO)	Sigma-Aldrich, Munich GER
Donkey Serum	Sigma-Aldrich, Munich GER
Dulbecco's PBS (1x w/o Ca^{2+}, Mg^{2+})	Invitrogen, Karlsruhe GER
Dulbecco's PBS (10x w/o Ca^{2+}, Mg^{2+})	Invitrogen, Karlsruhe GER
Essential Aminoacids (50x)	Invitrogen, Karlsruhe GER
Ethanol, abs.	Merck, Darmstadt GER
Fetal bovine serum	PAA, Linz Austria
Fluka H^2O, RNase/DNase free	Sigma-Aldrich, Steinheim GER
Fluorescence Mounting Media	Dako, Glostrup Denmark
Gentamycin (10mg/mL)	Invitrogen, Karlsruhe GER
Goat Serum	Sigma-Aldrich, Munich GER
HEPES 1M	Invitrogen, Karlsruhe GER
Horse Serum, heat inactivated	Invitrogen, Karlsruhe GER
Isopropanol	Merck, Darmstadt GER
L-Glutamin (200mM)	Invitrogen, Karlsruhe GER
Magnesiumchloride	Sigma-Aldrich, Steinheim GER
Methanol	Merck, Darmstadt GER
Methyl-Cellulose	Sigma-Aldrich, Munich GER
OCT-Media Tissue-Tec®	Leica Microsystems, Wetzlar GER
Paraformaldehyde	Sigma-Aldrich, Steinheim GER
PBS (1x w/o Ca^{2+}, Mg^{2+})	PAA, Linz, Austria
Penicillin-Streptomycin (10.000 U/mL each)	Invitrogen, Karlsruhe GER
Penicillin-Streptomycin (5000 U/mL, 5000µg/mL)	Invitrogen, Karlsruhe GER
Percoll	GE Healthcare, Uppsala Sweden
Poly-L-Lysine (0,1%)	Sigma-Aldrich, Munich GER
Potassiumchloride	Merck, Darmstadt GER
Sigmacote SL-2	Sigma-Aldrich, Munich GER

Sodiumchloride   Merck, Darmstadt GER

Triton X-100   Sigma-Aldrich, Steinheim GER

Tween   Cayman, Michigan USA

Trypan blue (0,4%)   Sigma-Aldrich, Munich GER

Ultrasonol 7, neutral   Roth, Karlsruhe GER

HEPES basal buffer for DRG stimulation (Ref.)

HEPES 25 mM   Invitrogen, Karlsruhe GER

Supplements:

135 mM   NaCl

3,5 mM   KCl

2,5 mM $CaCl_2$

1,0 mM $MgCl_2$

3,3 mM   Glucose

0,1 %   BSA

-               PH 7,4

HEPES high potassium for DRG stimulation

HEPES basal

Supplements:

50 mM   KCl

HEPES Capsaicin for DRG stimulation

HEPES basal

Supplements:

50nM   Capsaicin

2.3   Enzymes and Recombinant Proteins

Trypsin EDTA   PAA, Linz Austria

Collagenase   Invitrogen, Karlsruhe GER

Dispase II (2,4U/mL)   Roche, Penzberg GER

Human NGFβ   Sigma-Aldrich, Munich GER

Mouse NGF 7S   Merck, Darmstadt GER

2.4   Assays and Kits

BCA-Assay Uptima   Interchim, Montlucon France

Bioplex Cell Lysis Kit   Bio-Rad, Munich GER

NGFβ Single Plex Kit   Bio-Rad, Munich GER

Human CGRP EIA Kit   Cayman, Michigan USA

TaqMan 18s Gene Expression Assay   Applied Biosystems, Foster City USA

TaqMan high capacity cDNA RT Kit   Applied Biosystems, Foster City USA

TaqMan human NGFβ Gene Expression Assay   Applied Biosystems, Foster City USA

TaqMan universal PCR MasterMix   Applied Biosystems, Foster City USA

RNase free DNase Set   Qiagen, Hilden GER

RNeasy Mini Kit   Qiagen, Hilden GER

2.5   Cell Culture Media and Supplements

DMEM culture medium for primary fibroblasts (Gibco)

DMEM *high glucose (4,5g/L)* with phenolred   Invitrogen, Karlsruhe GER

Supplements:

10% v/v   Fetal bovine serum

10 µl/mL   Glutamax

50 U/mL   Penicillin

50 µg/mL   Streptomycinsulfate

DMEM cryomedium for primary fibroblasts (Gibco)

DMEM cryomedium with DMSO   Invitrogen, Karlsruhe GER

7,5 % v/v   DMSO

DMEM medium for dorsal root ganglion cell isolation (Sigma)

DMEM *high glucose* with Gentamycin   Sigma-Aldrich, Munich GER

Supplements:

5 µg/mL   Gentamycin (10mg/mL)

KGM-2 culture medium for primary keratinocytes (Lonza)

KBM-2 w/o Ca^{2+} Lonza, Walkersville MD USA

Supplements:

Bovine pituitary extract (BPE)

Epinephrine

Gentamycin, Amphotericin-B

Human epidermal growth factor (hEGF)

Hydrocortisone

Insulin

Transferrin

Ca^{2+} 0,1 mM

KGM-2 cryomedium for primary keratinocytes (Lonza)

KGM cryomedium with DMSO and fetal bovine serum   Lonza, Walkersville MD USA

20% v/v   Fetal bovine serum

7,5% v/v   DMSO

F12 culture media for primary dorsal root ganglion cells (Sigma)

F12 basal medium 500 mL   Sigma-Aldrich, Munich GER

Supplements:

10% v/v   Horse serum

10 ng/mL   Human NGFβ

1,5 mL   Essential aminoacids (50x)

2,5 mL   L-Glutamin (200 mM)

5 mL   Penicillin-Streptomycin (10.000 U/mL)

2.6   Plastic ware and Consumables

6 well plates	Greiner, Nürtingen GER
96 well plates	Greiner, Nürtingen GER
96 well optical reaction plate, MicroAmp	Applied Biosystems, Darmstadt
Adhesion films, MicroAmp	Applied Biosystems, Darmstadt
Bottle top filters (150mL, 250mL)	Nalgene, Lawrence KS USA
Cell culture dishes, 35mm x 10mm	Becton Dickinson (BD), USA
Cell culture flasks (25, 75, 185, 500 cm^2)	Greiner, Nürtingen GER
Cell strainer Nylon 70 μm	Becton Dickinson (BD), USA
Cover glass, 12 mm, 25 mm diameter	VWR, Darmstadt GER
Cover glass, rectangular	Menzel-Glass, Braunschweig GER
Cryotubes, 1,5 mL	Nunc, Wiesbaden GER
Dumont Nr.5 forceps	Reiss, Mainz GER
Eppendorf tubes (0,5, 1, 1,5 mL)	Eppendorf, Hamburg GER
Falcon tubes (15 mL, 50 mL)	Greiner, Nürtingen GER
Glass syringe, Luer lock 2 mL	Fortuna Optima, Wertheim GER
Latex gloves powder free	Kimberly-Clark, Mainz GER
Needles, 21 gauge	Unimed, Lausanne CH
Neubauer chamber and cover glass	Brand, Wertheim GER
Pasteur pipettes, plugged and non-plugged	VWR, Darmstadt GER
Sterile biopsy instruments (scissors, forceps)	Aesculap, Hammacher GER
Superfrost microscope slides	Menzel-Glass, Braunschweig GER
Super PAP pen, large	EMS, Munich GER

2.7   Equipment and Instrumentation

Analytical balances

BP211D precision balance	Sartorius, Göttingen GER

Autoclaves

Varioklav 135S	H+P, Oberschleißheim GER
Technoklav	IBS integra biosciences, Chur CH

Bioplex System

    Bioplex 2200 System   Bio-Rad, Munich GER

Cell Couting devices

    Neubauer hemocytometer   Schreck, Hofheim GER

    Nucleo Counter   Chemometec, Gydevang Denmark

Centrifuges

    Centrifuge 5415 R   Eppendorf, Hamburg GER

    Heraeus Megafuge 1.0R   ThermoScientific, Schwerte GER

    Heraeus Multifuge3 S-R   ThermoScientific, Schwerte GER

Cooling units

    -196°C Cryostorage System K10   Taylor-Wharton Theodore, AL USA

    -80°C ultra low temperature freezer   Liebherr, Ochsenhausen GER

    -20°C freezer   Liebherr, Ochsenhausen GER

    +4°C refrigerator   Bosch, Munich GER

Cryotom

    Leica CM3050S   Leica Microsystems, Wetzlar GER

Ice machine

    ZBE 30-10   Ziegra-Ice machines, Isernhagen GER

Incubators

    HERAcell 150   Heraeus, Hanau GER

    HERAcell 240   Heraeus, Hanau GER

Lamina Flow Workbenches

    HERAsafe KS 12   Kendro, Hanau GER

    HERAsafe   Kendro, Hanau GER

Magnetic stirrers and heating plates

    Big Squid   IKA-Works, Staufen GER

    VMS C4   VWR, Darmstadt GER

Microscopes

    Axiovert S100   Zeiss, Göttingen GER

    Confocal Laser Scanning Microscope   Olympus, Hamburg GER

    Leica MZ6   Leica Microsystems, Wetzlar GER

    MCX 1600   Micros, Vienna Austria

Orbital shaker

    Thermo mixer comfort, plate shaker   Eppendorf, Hamburg GER

    MS 1 Minishaker   IKA, NC USA

PCR machines

    DNA Engine   Biozym, Oldendorf GER

    7900 HT Fast Real-Time PCR System   Applied Biosystems, Foster USA

pH-Meter

    763 Multi-Calimatic   Knick, Berlin

Photometer

    Spectra Max 250   Molecular Devices, Sunnyvale USA

    Nanodrop ND-1000   Peqlab, Wilmington USA

Pipettes

Micropipettes

    Reference 0,5-10 µL   Eppendorf, Hamburg

    Reference 0,5-20 µL   Eppendorf, Hamburg

    Reference 10-100 µL   Eppendorf, Hamburg

    Reference 100-1000 µL   Eppendorf, Hamburg

    Reference 500-2500 µL   Eppendorf, Hamburg

Multichannel pipettes manual

    Finpipette manual (12-channel) 50-300   Labsystems, Helsinki Finland

    Finpipette manual (8-channel) 50-300   Labsystems, Helsinki Finland

    Finpipette manual (8-channel) 5-50   Labsystems, Helsinki Finland

    Pipetboy acu   IBS Integra Biosciences, Chur CH

Vacuum System and Suction devices

    Vacusafe comfort   IBS Integra Biosciences, Zurich CH

    Miniport   Hassheider, Köln GER

Water purification system

    Milli-Q academic   Millipore, Eschborn GER

Water baths

    GFL 1002   GFL, Burgwedel GER

2.8   Cell Material

Human cell material was derived from skin biopsies supplied by clinical cooperation partners. The average age of donors was 56,6 years, ranging from 34 to 74 years. Upon removal, skin biopsies were immediately cooled (4°C), placed on DMEM soaked membranes and subjected to the isolation of dermal fibroblasts and epidermal keratinocytes the same day.

Dorsal root ganglion cells were isolated from porcine spines (*sus scrofa domestica*) kindly provided by the lab of Prof. Dr. Martin Schmelz, University of Heidelberg. The spine of piglets was removed between postnatal day 2 and 5, cleaned with ice cold PBS, cut in half and stored in pre-cooled (4°C) DMEM. The samples were kept on ice during transportation and the subsequent isolation of dorsal root ganglia.

2.9   Software

AnalySIS® Version 3.2	Soft Imaging System, Münster GER
AxioVision Version 4.7	Zeiss, Göttingen GER
Bioplex Manager	Bio-Rad, Hercules USA
Graphpad Prism 4	Graphpad Software, San Diego USA
ImageJ	http://rsbweb.nih.gov/ij/
Leica for CLSM	Olympus, Hamburg GER
ND-1000 V3.3.0	Peqlab, Wilmington USA
RQ Manager 1.2	Applied Biosystems, Foster USA
SDS 2.3 analysis software	Applied Biosystems, Foster USA
SoftMax Pro Version 2.0.1	Molecular Devices, Suuyvale USA

3 Methods

3.1 Cell Biology

All Cell Biology techniques were performed under sterile conditions. Cell material employed for *in-vitro* and co-culture experiments comprised of keratinocytes ≤ passage 3 and fibroblasts ≤ passage 4 isolated from human skin biopsies, as well as dorsal root ganglion cells (DRGs) derived from porcine spines (*sus scrofa domestica*).

3.1.1 Isolation and cultivation of human keratinocytes and fibroblasts

Until the isolation of keratinocytes and fibroblasts human skin biopsies were cooled (4 °C) and nurtured by a DMEM soaked membrane. First, subcutaneous and adipose tissue were removed and the biopsies were cut into small pieces of 3 mm edge length. Following a short disinfection in 70 % ethanol and PBS with penicillin and streptomycin (50 U/mL, 50 µg/mL), the biopsy pieces were subjected to 2 hours of enzymatic digest in dispase-II (2 U/mL) at 37 °C. The epidermis was subsequently stripped off the dermis, incubated additional 10 min in 1x Trypsin (PAA) at 37 °C and then pressed through a 70 µm cell strainer. Dissociated keratinocytes were collected, resuspended in KGM-2 (Lonza) and seeded into 75 cm^2 cell culture flasks. Medium was changed every second day and cells were transferred into the next bigger cell culture flask after reaching 80 % confluence.

The dermis was placed into the cavities of a 6-well plate. After becoming adherent, the pieces were covered with DMEM (Gibco) and cultivated at 37 °C in 5 % CO_2. Until the outgrowth of fibroblasts, medium was changed every 4-5 days, later every 2-3 days. After reaching confluence, the dermis pieces were removed and the fibroblasts were seeded into cell culture flasks.

3.1.2 Cell counting of primary skin cells

The cell count of primary keratinocytes and fibroblasts was determined previously to cryopreservation and seeding into co-culture chambers or 6-well plates. Skin cells were trypsinized and resuspended in KGM-2 (Lonza) or DMEM (Gibco), respectively. The cell count was determined using a Neubauer chamber. To exclude dead cells from count, Trypan blue was added in a 1:1 ratio. The missing integrity of dead cell membranes allows the diffusion of the dye into the cytoplasm, thus the discrimination between viable and dead cells.

3.1.3 Cryopreservation of primary skin cells

1x10^6 cells were resuspended in 1 mL of keratinocyte or fibroblast cryomedium. Cells were gradually frozen in isopropanol chambers at −80 °C and stored at −196 °C in a cryostorage system.

For resuspension cell vials were quickly thawed at 37° C and immediately seeded into 75 cm^2 cell culture flasks at a density of approximately 1x10^4 cells per cm^2. To limit the effect of cryomedium supplements as DMSO, medium was changed the following day.

3.1.4 Isolation and cultivation of porcine dorsal root ganglion cells (DRGs)

The spine of piglets was removed, cleaned with ice cold PBS, cut in half and stored in pre-cooled (4 °C) DMEM. The samples were kept on ice during excision and subsequent cleaning of dorsal root ganglia. D-PBS without Ca^{2+} Mg^{2+} was used for all washing steps.

Each piece of spine was cut in half along the medial axis and the dorsal root ganglia were excised from both sides of the vertebral canal. A binocular microscope was used to remove the ventral and dorsal axonal radices, as well as the dura mater. Cleaned DRGs were transferred to collagenase (740 U/mL in DMEM with Gentamycin) and incubated 3x 45 min at 37°C. Every 45 min half of the collagenase solution was replaced. Following two washing steps the DRGs were subjected to an additional 10 min of digest in 1x Trypsin (PAA) at 37 °C. DRGs were subsequently dissociated using a coated, fire polished Pasteur pipette. The cells were separated from fiber material of the extracellular matrix by Percoll density gradient centrifugation (20 % Percoll) and resuspended in F12 with 10 ng/mL human NGFβ (huNGFβ).

The cell count was determined using a NucleoCounter. 16x10^4 dorsal root ganglion cells were seeded into the middle compartment of a co-culture chamber and cultivated at 37 °C in 5 % CO_2. Medium was changed every second day.
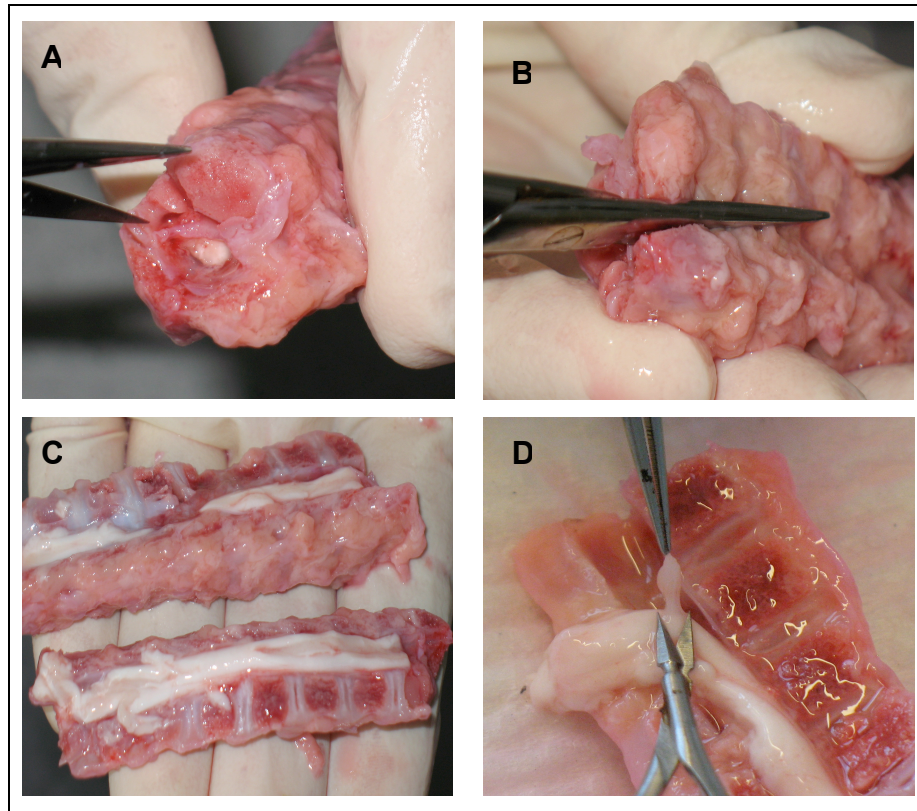
Figure 5: Excision of the DRGs of a porcine spine
A) – C) The spine is cut in half along the medial axis. **D)** DRGs are excised from the vertebral canal.

3.1.5   Cell counting of DRGs via NucleoCounter

DRGs compose of a heterogeneous mixture of sensory neuron cell bodies of different size associated with small glial cells, often referred to as satellite cells. To obtain an exact, reliable and reproducible cell count for dissociated dorsal root ganglion cells ChemoMetec's NucleoCounter was used.

The NucleoCounter is basically a fluorescence microscope with an integrated optical imaging and analysis system. It accounts for different cell size, cell viability and errors due to the aggregation of cells, by cell lysis and by counting the fluorescent labeled nuclei.

A small sample volume of 50 µL is subjected to lysis by low pH (solution A), followed by a stabilizing solution B. The mixture is sucked into the NucleoCasette, a small device combining flow channels with immobilized propidium iodide and a measurement chamber of defined volume. Propidium iodide intercalates between the base pairs, is excited by green light of 535 nm and emits red light of 617 nm. The NucleoCounter determines the total amount of fluorescent nuclei in the measurement

chamber. Correction for cell viability is achieved by measuring the amount of nuclei and therefore dead cells, labelled in non-lysed cell suspension.

Equal volume of dissociated DRG cell suspension, solution A and solution B were mixed and subsequently sucked into the NucleoCasette. The number of viable cells was obtained from measuring the untreated DRG cell suspension, and subsequent subtraction from the total DRG cell count.

3.1.6   Co-culture model of human skin cells and porcine DRGs

In-vivo the peripheral terminals of sensory neurons in the skin are clearly separated from their cell bodies in the dorsal root ganglia and thus located in a completely different microenvironment. This particular anatomical and physiological feature constitutes a major drawback in the development of accurate *in-vitro* models of the peripheral sensory network of the skin.

Two major problems are to be solved: First, the peripheral axonal fibers and their cell bodies have to be spatially separated. Second, non-neuronal cells in the periphery e.g. skin cells require cultivation media different from medium optimized for dorsal root ganglion cells.

In cooperation with the lab of Prof. Dr. Martin Schmelz, Ruprecht-Karls University of Heidelberg, a culture chamber was developed that allows the cultivation of neuronal somata and their axonal processes in separate compartments. Due to a silicon seal that is largely impermeable to liquids between these compartments, the co-cultivation of skin cells within the axonal "peripheral" compartment was possible.

Cultivation-chambers were prepared 2-3 days before the isolation of the DRGs and stored at 4 °C until testing the leak tightness of the seal. 6-well plates were coated with poly-L-lysine (0,1 %) over night, washed with sterile PBS and dried at RT. Using a metal ridge, parallel grid lines spaced 300μm apart were scratched into the coated surface of each 6-well cavity. Two parallel lines of a sugar polymer were subsequently applied rectangular to the scratched grid lines. Sterile silicone was applied on the edges of co-culture chambers using a glass syringe with a 21-gauge needle. The chambers were subsequently placed into the cavities of the 6-well plate, on top of the sugar polymer.

A sterile weight of approximately 300 g was placed on top of the chambers for several seconds to generate a tight seal between the chamber compartments. Following 1 h of sterilization under UV-light at RT, the middle compartment was filled with F12

medium (Sigma) and placed at 37 °C over night. Thus, leaky chambers excluded from subsequent experiments.

16×10^4 dissociated dorsal root ganglion cells were seeded into the middle compartment and cultivated in F12 (Sigma) with 10 ng/mL huNGFβ. Following over night incubation and adherence of DRGs, chambers were again checked for impermeable seals. Subsequently, the "peripheral" side chambers were loaded with the respective potential axonal growth cues, NGFβ or skin cells. Loading of the side chambers stated time point d = 0 of the cultivation period. Co-culture chambers were cultivated for 10 days at 37 °C in 5 % CO_2. The medium of each compartment was changed every second day.
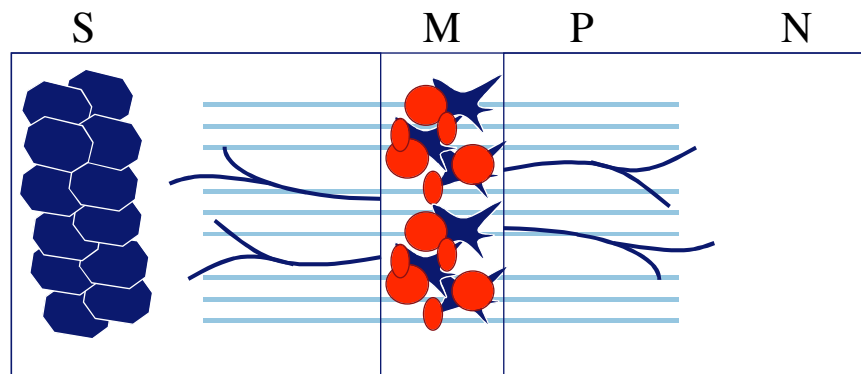
Figure 6: Sketch of the co-culture chamber
DRGs are seeded into the middle compartment (M), axonal processes extend into the peripheral side compartments (P) guided by grid lines (light blue). Growth cues: neurotrophic factor NGFβ (N), skin cells (S)
(S) skin cells, (M) middle chamber, (P) peripheral chamber, (N) neurotrophic factors

3.2 Induction and manipulation of peripheral nerve fiber growth

The principle of the co-culture chamber is based on eliciting peripheral axonal fiber growth in the side compartments, whereas the dorsal root cell bodies are cultivated in the middle chamber. Notably, cultivation conditions in the middle chamber were optimized for DRGs, whereas side chambers were loaded with potential growth cues. Fiber outgrowth induced by huNGFβ, skin cells and conditioned media was investigated. Respective cultivation media only (KGM-2, DMEM, F12) served as negative controls and experiments were run in duplicates. Co-culture chambers were cultivated for 10 days at 37 °C in 5 % CO_2. The medium of each compartment was changed every second day.

Peripheral fiber growth was observed using an optical microscope on day 4 or 5, day 6 and day 10. Pictures of each neurite in the side chamber were taken and subjected to analysis (see 3.3).

3.2.1   Effect of external human NGFβ on peripheral fiber growth

Due to its well-characterized neurotrophic effect on peripheral sensory neurons, huNGFβ was used to set up and evaluate the co-culture system. Increasing concentrations of NGFβ, 0,04 ng/mL, 0,2 ng/mL, 1 ng/mL, 5 ng/mL and 10 ng/mL in F12 (Sigma), were loaded into the side compartments of co-culture chambers.

3.2.2   NGFβ sequestration via anti-NGFβ antibody

To selectively block the growth of neurites mediated by huNGFβ, an affinity purified anti-NGFβ antibody (R&D) was applied. This antibody was developed to block the biological activity of NGFβ, as previously shown in an ^{3}H-thymidine incorporation assay with TF-1 cells [91].

To investigate the inhibition of the biological activity of NGFβ, both NGFβ and anti-NGFβ antibody were mixed in the side compartments. 2μg/mL antibody and 10 ng/mL huNGFβ in F12 (Sigma) were incubated for 10 min at RT prior to loading. Growth of peripheral fibers was monitored and analyzed as described in 3.3.

Additionally, a complexation assay was conducted, to detect free, non-sequestered NGFβ in solution using the Bioplex assay (3.7.2). 10 ng/mL huNGFβ in F12 (Sigma) were mixed with increasing concentrations of anti-NGFβ antibody: 0,01 μg/mL, 0,05 μg/mL, 0,1 μg/mL, 1 μg/mL and 2 μg/mL. Following 15 min incubation at RT the remaining amount of NGFβ in solution was quantified with a Bioplex assay.

3.2.3   Effect of primary skin cells on peripheral fiber growth

To investigate the ability of primary skin cells to induce peripheral fiber growth, keratinocytes and fibroblasts were seeded into the side compartment of the co-culture chambers.

Skin cells were trypsinized and resuspended in KGM-2 (Lonza) or DMEM (Gibco), respectively. The cell count was determined using a Neubauer hemocytometer. 1x10^4 cells were seeded close to the border of the side compartment using a sterile insert. In parallel, supernatants of the side compartments were subjected to NGFβ Bioplex assays to determine the amount of secreted NGFβ. Every second day

previously to the change of the media, supernatants were collected and stored at −80 °C until NGFβ quantification.

3.2.4 Effect of NGFβ sequestration in supernatants of primary skin cells

To selectively neutralize the effect of NGFβ secreted by primary skin cells, an affinity purified anti-NGFβ antibody (R&D) was applied, as described in 3.2.2.

Using the NGFβ concentration measured in the supernatants of keratinocytes and fibroblasts as a guide value, 0,1 µg/mL antibody were applied to equal an approximately 1000-fold excess of antibody to its epitope. The successful complexation of free NGFβ by the antibody was controlled using a Bioplex assay. Every second day previously to the change of the media, supernatants were collected and stored at −80 °C until NGFβ quantification.

3.2.5 Effect of conditioned media of primary skin cells on peripheral fiber growth

It was investigated, whether conditioned media of keratinocytes and fibroblasts are able to mimic the effect of primary skin cells seeded into the side compartments.

Medium of skin cells cultured for two days in 185 cm^2 culture flasks exhibiting > 80% confluence was collected and stored at −80 °C. Conditioned media were subjected to 5 min centrifugation at 10.000 rpm directly before being loaded into the side compartments.

3.2.6 Effect of NGFβ sequestration in conditioned media of primary skin cells

To selectively inhibit the effect of secreted NGFβ in conditioned media, an affinity purified anti-NGFβ antibody (R&D) was applied, as described in 3.2.2.

The NGFβ concentration measured in conditioned media of keratinocytes and fibroblasts served as guide values to determine the antibody concentration that equals an approximately 1000-fold excess of antibody to its epitope. The successful complexation of free NGFβ was controlled using a Bioplex assay.

Conditioned medium and 0,1 µg/mL antibody were incubated for 15 min at RT previously to loading of the side compartments and determination of the free NGFβ content.

3.3 Monitoring and analysis of peripheral fiber growth

Peripheral fiber growth was observed on day 4 or 5, day 6 and day 10 with an optical microscope. Pictures of each process or several mosaic pictures of adjacent areas of the side comparment were taken using AxioVision 4.7 software. Thus, double counts of processes were avoided.

Subsequent analyses of fiber length were conducted with ImageJ and AnalySIS® Version 3.2. Total peripheral fiber growth of a given side compartment was determined as the sum of the length of each individual grown fiber in µm, termed cumulative peripheral neurite length (CPNL). Occasional reanalysis of random chosen data sets were conducted and revealed similar results.

Figure 7: Analysis of total growth of peripheral fibers. 100µm were used as reference scale to determine the pixel / µm ratio.

	Mean	Min	Max	Angle	Length
1	152,160	127	255	0	156
2	115,028	7,277	240,084	0	358,471
3	129,701	77,235	199,311	0	110,469
4	119,702	22,309	180,305	0	96,363
5	107,724	6,546	255	0	281,771
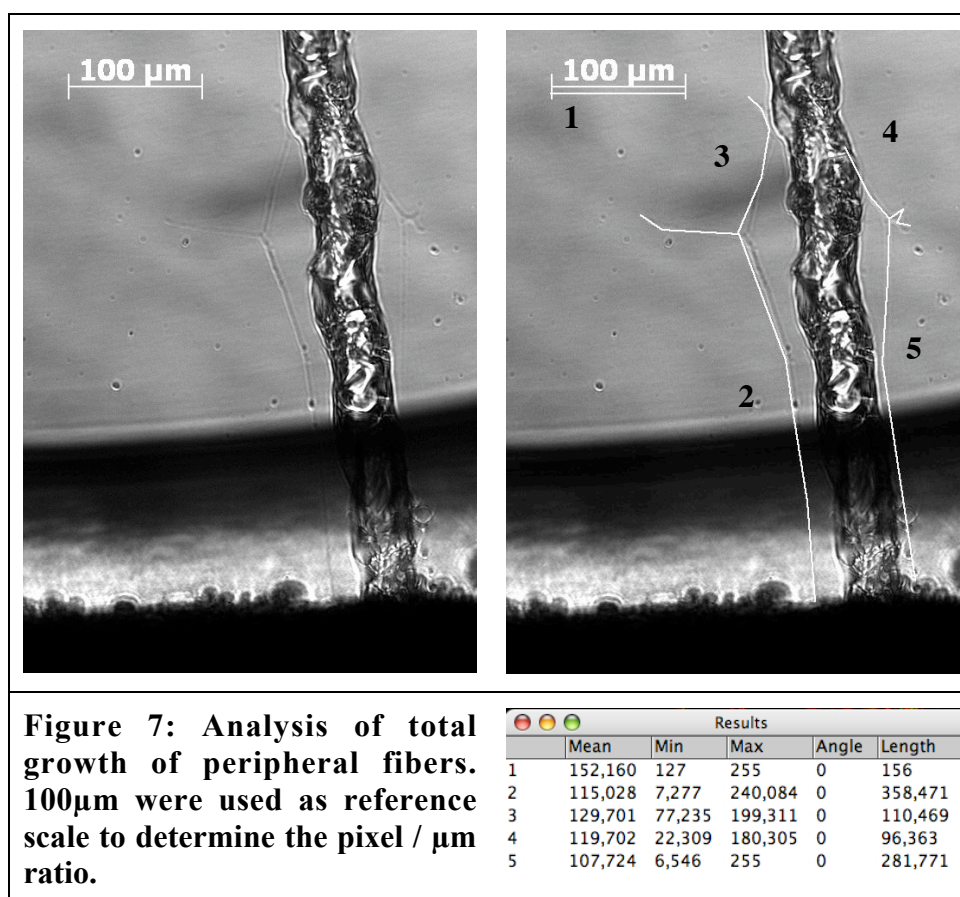
3.3.1 Immunofluorescence (IF) staining of DRGs and primary skin cells in co-culture

Peripheral fibers in co-culture with skin cells were subjected to immunofluorescence (IF) staining for histological identification on day 10. Keratinocytes were stained with anti-wide-spectrum cytokeratin antibody (Abcam) [92], fibroblasts with anti-fibroblast surface protein antibody (Abcam) [93] and axonal processes were stained using the pan axonal neurofilament marker SMI312 (Covance) [94]. IF staining was conducted as described in 3.4.1.

List of Antibodies	**Dilution**	**Source**
Rabbit polyclonal anti-wide spectrum Cytokeratin	1:1000	Abcam
Mouse monoclonal anti-Fibroblast Surface Protein	1:200	Abcam
Mouse monoclonal anti-Pan-Axonal Neurofilament	1:2000	Covance
Alexa Fluor 488, Goat anti-rabbit IgG (H+L)	1:1000	Mol.Probes
Alexa Fluor 488, Goat anti-mouse IgG (H+L)	1:1000	Mol.Probes
Alexa Fluor 594, Goat anti-mouse IgG (H+L)	1:1000	Mol.Probes

3.4 Characterization of nociceptive DRGs via IF staining

The nociceptive phenotype of dorsal root ganglion cells and their peripheral fibers was displayed using the nociceptive, peptidergic markers calcitonin-gene-related-peptide (CGRP) and the receptor tyrosine kinase TrkA, the non-peptidergic marker Isolectin B4 (IB4) and the ambiguously expressed vanilloid receptor TRPV1. IF staining of DRG somata in the middle compartment, as well as their peripheral fibers in the side compartment was conducted.

Monitoring and analysis of peripheral fibers and their respective marker expression was performed as described in 3.3. The fraction of peripheral fiber length expressing each marker compared to total fiber growth was investigated. Individual fractions of marker expression were stated as percentage of cumulative peripheral neurite length (CPNL).

List of Antibodies	**Dilution**	**Source**	**Ref.**
Mouse monoclonal anti-Pan-Axonal Neurofilament	1:2000	Covance	[94]
Rabbit polyclonal anti-PGP9.5	1:1000	Abcam	[95]
Mouse monoclonal anti-CGRP	1:500	Abcam	[96]

List of Antibodies	Dilution	Source	Ref.
Rabbit polyclonal anti-TrkA	1:200	Abcam	[97]
Rabbit polyclonal anti-TRPV1	1:200	Abcam	n.d.
Isolectin GS-IB4, Alexa Fluor 488 conjugate	1:200	Mol.Probes	[98]
Alexa Fluor 594, Goat anti-mouse IgG (H+L)	1:1000	Mol.Probes	
Alexa Fluor 594, Goat anti-rabbit IgG (H+L)	1:1000	Mol.Probes	
Alexa Fluor 488, Goat anti-mouse IgG (H+L)	1:1000	Mol.Probes	
Alexa Fluor 488, Goat anti-rabbit IgG (H+L)	1:1000	Mol.Probes	

3.4.1   Immunofluorescence (IF) staining of DRGs

Primary and secondary antibodies were diluted in PBS with 1 % goat serum and all steps were carried out at RT, if not stated otherwise.

Co-culture chambers were carefully washed with PBS and the cells were fixed in 4 % Paraformaldehyde (PFA) for 15 min. Following two washing steps, cells were permeabilized in 0,1 % Triton in PBS (PBS-T) for 10 min. After two additional washing steps, 1 hour of incubation with blocking solution (1 % BSA) took place. Primary antibodies were diluted directly before use and over night incubation was carried out at 4 °C in humid chambers.

Subsequently, chambers were washed with 1 % goat serum in PBS and subjected to 3 hours of secondary antibody incubation at RT in the dark. Following two washing steps with 1 % goat serum in 0,1 % PBS-T and a third with PBS only, DAPI solution was applied for 15 min. Chambers were washed with PBS and subjected to increasing concentrations of ethanol (50 %, 70 %, 96 %). The co-culture chambers were carefully removed using surgical blades. Fluorescence Mounting Media (Dako) and coverslips of 25 mm diameter were used for mounting. 6-well plates were allowed to dry over night at 4 °C before examination under the microscope.

3.5   Determination of the functionality of DRGs

To determine whether cultured DRGs and their peripheral fibers are functional and therefore can be stimulated to release neurotransmitter, a modified version of the stimulation assay employed by Hingtgen in 2006 was conducted [99]. In rats, CGRP is expressed in over 40 % of peptidergic DRGs and therefore comprises the most abundant neuropeptide. Hence, CGRP release upon stimulation was chosen as readout parameter.

To examine, whether stimulation of DRG somata in the middle compartment is transmitted to the side compartment, stimuli application was restricted to the middle chamber. Neuropeptide secretion was detected in the middle and side compartment, respectively.

Co-culture chambers cultivated in the presence of 10 ng/mL huNGF were subjected to stimulation at day 10. Two subsequent stimulation cycles were conducted to examine repetitive stimulation. The incubation period was set to 10 min at 37 °C in 5 % CO_2. After every period supernatants were collected and stored at –20 °C until detection of CGRP concentrations (3.7.1).

At the start of each cylce, chambers were carefully washed with HEPES buffer. To determine basal CGRP release, the cultures were initially incubated with HEPES. Subsequently, stimuli were applied to the middle compartments, whereas HEPES is loaded into the side compartments. Following careful washing steps, a second stimulation cycle was performed.

Figure 8: Scheme of the stimulation assay
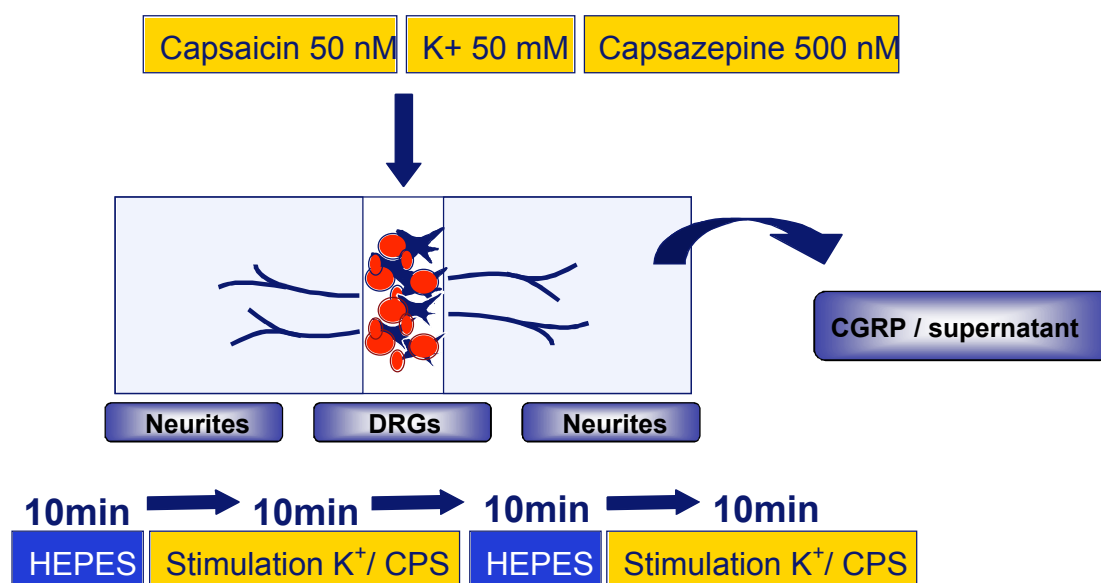Respective stimuli (high potassium, 50 mM; TRPV1 agonist capsaicin, 50 nM) and the specific TRPV1 antagonist capsazepine (500 nM) are applied to the middle compartment alone and in various combinations; Secreted CGRP is detected in the supernatants of the side and middle compartment by EIA. 1 cycle of stimulation comprises 10 min incubation with HEPES, followed by 10 min stimulation.

First, stimulation with 50 mM potassium was used to unspecifically cause depolarization and neurotransmitter release of the DRGs. Second, a specific, ligand-receptor mediated stimulation was performed using the TRPV1 agonist capsaicin (CPS). TRPV1 is expressed in a subpopulation of DRGs *in-vivo*, as well as in culture (examined in 3.4). 50 nM capsaicin in HEPES basal were applied.

To assess the potential of the system to specifically block the ligand-receptor mediated stimulation, the synthetic TRPV1 antagonist capsazepine (CPZ) was co-applied with CPS and high potassium, respectively. Capsazepine was employed in a 10-fold excess over capsaicin at a concentration of 500nM and was co-applied with 50 mM potassium.

3.6 Immunohistochemistry

Punch biopsy material of normal and atopic human skin was derived from clinical cooperation partners. Following excision biospies were rinsed with PBS, mounted in Tissue-Tec® and subjected to cryopreservation in liquid nitrogen. Biopsy material was stored at −80 °C until preparation of cryosections.

3.6.1 Cryosections human skin

Vertical sections of 5 μm and 50 μm were genereated using a Leica CM3050S cryotom. 4 to 5 sections were transferred to one microscope slide. The sections were dried for 1 hour at RT and subsequently fixed with icecold aceton. Sections were stored at −20 °C until immunofluorescence staining.

3.6.2 Immunofluorescence (IF) staining of skin cryosections

Anti-pan-axonal neurofilament antibody SMI312 (Covance) was used to monitor peripheral neuronal structures in normal and atopic skin. Epidermal structures were stained with anti-cytokeratin 1/10 antibody (Covance). All antibodies were diluted in 1 % BSA.

Aceton fixed cryosections were washed with PBS and blocked with 3 % BSA for 1 hour at RT. Primary antibody incubation was performed over night at 4 °C using a humid chamber. The next day sections were washed with 0,1 % Triton in PBS (PBS-T), followed by PBS only. Subsequent secondary antibody incubation took place for 2 hours at RT in the dark. After another washing step with PBS sections were subjected to DAPI staining for 15 min at RT, followed by dehydration using

increasing concentrations of ethanol (50 %, 70 %, 96 %). Sections were mounted with fluorescent mounting media (Dako) and dried over night at 4 °C.

List of Antibodies	Dilution	Source	Ref.
Mouse monoclonal anti-Pan-Axonal Neurofilament	1:2000	Covance	[94]
Rabbit polyclonal anti-Cytokeratin 1/10	1:1000	Covance	n.d
Alexa Fluor 594, Goat anti-mouse IgG (H+L)	1:1000	Mol.Probes	
Alexa Fluor 488, Goat anti-rabbit IgG (H+L)	1:1000	Mol.Probes	

3.7　Protein Biochemistry

3.7.1　Quantitative analysis of CGRP

To detect the concentration of CGRP released by DRG stimulation, a human CGRP Enzyme Immunoassay Kit (Cayman) was used. This EIA is based on a sandwich-enzyme-immunoassay. The 96-well plate is precoated with mouse monoclonal anti-CGRP antibody that captures free CGRP protein. The acetylcholinesterase (AChE) conjugated tracer (Fab') binds specfically to a different epitope of CGRP. The enzymatic activity of AChE hydrolyzes an ester bond of the added Ellman's reagent, forming a yellow compound. The intensity of the color is proportional to the amount of CGRP. The absorbance is measured at 405 nm, unspecific absorption was detected at 650 nm. The limit of detection is stated with 2 –5 pg/mL.

Precoated plates were washed 5 times with washing buffer. 100 µL of Ellman's reagent, medium (for non-specfic binding), standards (1000 pg/mL – 7,81 pg/mL) and samples were employed. 100 µL of anti-CGRP AChE tracer were added except for cavities with blank. Following 20 hours of incubation at 4 °C and several washing steps, 200 µL of Ellman's reagent was added. Absorbance is measured after 60 min of incubation at RT.

3.7.2　Quantitative analysis of NGFβ via Bio-Plex assay

To detect the concentration of NGFβ in supernatants of co-culture chambers, in conditioned media and in the supernatants of primary skin cells, a Bio-Plex Cytokine Assay was used. In general it is possible to quantitatively detect 27 different cytokines and growth factors in parallel in one sample.

This assay is based on the simultaneous detection of the identity and the quantity of a protein of interest. Notably, an optimized flow cytometer with two lasers and a high-speed signal processor is necessary. The solid phase of an ordinary EIA is replaced by fluorescence color coded microbeads that are covalently bound to the capture antibodies. The color code of the microbead is clearly identified by the laser system of the flow cytometer and designates the protein type.

A secondary biotinylated antibody recognizes a different epitope of the protein of interest. Streptavidin-Phycoerythrin is added and binds the biotinylated detection antibody. The intensity of the fluorescent signal after excitation at 532 nm, compared to a standard curve determines the quantity of the protein.

The 96-well microplate was pre-wet with assay buffer. After each step, the liquid was removed by using vacuum filtration. The multiplex bead solution was added to each well, followed by washing steps. 50 µL of standard and samples were added and incubated for 30 min at RT. Following washing steps the detection antibody was added to each well and incubated for 30 min at RT. After an additional washing step, streptavidin-PE was applied to each well, followed by another 10 min of incubation. Finally, beads were resuspended in assay buffer and immediately subjected to detection.

3.7.3 Determination of total protein concentration

The concentration of NGFβ detected in the supernatants of primary skin cells (see 3.7.4.) was normalized to total protein concentrations.

The cells were lysed with cell lysis buffer (Biorad) with protease inhibitors and subjected to the BCA Protein Quantification Kit (Uptima). This colorimetric assay is based on an improved Biuret reaction. Cu^{2+} are reduced to Cu^{+} by oxidation of peptide bonds. Cu^{+} ions are subsequently bound by the specific chelator Bicinchoninic acid and form a water soluble purple complex. Absorbance at 562 nm is proportional to the protein concentration, which is determined using a standard curve.

Standards and samples are measured in triplicates. 5 µL of blank (lysis buffer), standards (2 mg/mL – 0,062 mg/mL) and samples were mixed with 200 µL of BCA reagent and incubated for 30 min at 37 °C. Absorption was measured at 562 nm using the Spectra Max 250 (Molecular Devices).

3.7.4 Expression and secretion of NGFβ in primary skin cells

To investigate the expression and secretion of NGFβ by keratinocytes and fibroblasts, the following assays were conducted.

3×10^4 primary skin cells were seeded into 6-well chambers and cultivated for 10 days at 37 °C in 5 % CO_2. Supernatants were collected at day 2, 4, 6 and 10. Samples were stored at −80 °C until the detection of NGFβ with the Bioplex Assay, as described in 3.7.2. In parallel skin cells were lysed using cell lysis buffer (Biorad) with protease inhibitors and total protein concentrations were detected using the BCA assay (3.7.3). The NGFβ concentration of the supernatants was normalized to the total protein concentration.

In a second setup skin cells were lysed using a guanidine-thiocyanate containing buffer (Qiagen) and subjected to mRNA isolation at day 2, 4, 6 and 10. Total mRNA was isolated with Qiagen spin columns (3.8.1) and subjected to reverse transcription using the TaqMan high capacity cDNA RT Kit (3.8.2). Expression levels of NGFβ were detected with real time PCR using the TaqMan human NGFβ Gene Expression Assay (3.8.3).

3.8 Molecular Biology

3.8.1 RNA isolation of primary skin cells

Skin cell lysates collected as described in 3.7.4 were subjected to mRNA isolation using the Qiagen RNeasy-Kit. This kit selectively excludes RNAs smaller than 200 nucleotides. Lysates were mixed with 70 % ethanol and transferred to RNeasy spin columns. RNA efficiently binds the silica-based membrane of the columns. The supernatant was removed by short centrifugation. Co-isolated DNA was degraded with DNase, followed by washing steps. mRNA was eluted in 50 µL of RNase free water and subjected to quantification and quality testing using a nanodrop ND1000 photometer (Peqlab). At neutral pH an absorbance of 1 at 260 nm correlates with 44 µg of RNA per mL. A ratio of 260 nm to 280 nm between 1.9 and 2.1 refers to comparatively pure RNA. The mRNA samples were stored at −80 °C until reverse transcription.

3.8.2   cDNA RT-PCR

1 µg of mRNA is conducted to reverse transcription in a total volume of 100 µL using the TaqMan high capacity cDNA RT Kit (Applied Biosystems). Per reaction 10 µL RT buffer, 4 µL dNTPs, 10 µL primer and 5 µL of reverse transcriptase were employed.

PCR Program for RT-PCR

25 °C   10 min

37 °C   120 min

4 °C $\propto$

3.8.3   TaqMan® realtime PCR

Expression levels of NGFβ mRNA were detected by real time PCR using the TaqMan human NGFβ Gene Expression Assay (Applied Biosystems). In parallel, expression of the endogenous control 18S rRNA was determined. Expression levels of NGFβ mRNA were normalized using the respective levels of 18S rRNA. Experiments were run in duplicates.

Assay   Catalog Number

NGFβ   Hs00171458_m1

18S   Hs99999901_s1

The TaqMan® system is based on a DNA probe with the fluorsecent reporter FAM™ bound to the 5 prime end and the quencher NFQ™ bound to the 3 prime end. The probe binds its complementary sequence within the amplified region between the primer pairs. During amplification the Taq polymerase degrades the probe. Both fluorscent reporter and quencher are released. Due to the lack of proximity of the quencher to the reporter, a fluorescent signal can be detected. Excitation of the fluorescent signal is achieved at 488 nm and emission takes place at 518 nm. Therefore, fluorescence intensity correlates with copy numbers of the amplified sequence.

3,5 µL of each primer pair were mixed with 33,5 µL Universal PCR Mastermix (Applied Biosystems). 3 µL of cDNA and 30,5 µL RNsae-free water were added and mixed. 25 µL total reaction volume was employed. 30 cycles of amplification were run and PCR protocol is indicated below.

PCR Program for TaqMan® PCR

50 °C	2 min	
95 °C	10 min	
95 °C	15 sec	30x
60 °C	60 sec	
4 °C	∝ sec	

Relative quantification is achieved by calculating ΔCT and RQ ($2^{-\Delta\Delta ct}$) from measured CT values according to the following scheme:

Value	Calculation
CT	Cycle threshold
ΔCT	$CT_{NGF\beta} - CT_{18S}$
$\Delta\Delta CT$	$CT_{NGF\beta} - CT_{18S} - \Delta CT_{Ko}$
RQ	$2^{-\Delta\Delta ct}$

3.9 Statistics

Statistical analysis was conducted using Graphpad Prism 4. Data were analysed assuming sampling from Gaussian distribution. Statistical tests included matched one and two-tailed t-tests, repeated measures one-way ANOVA for comparison of three or more matched groups, as well as two-way ANOVA for comparison of three or more groups analyzed for two or more conditions. Appropriate post tests included Dunnett's test to compare several groups to control, a test for linear trend and the Bonferroni test for selected pairs of groups. All values are stated as arithmetic mean ± standard deviation (SD). Significances are reported according to the following definition:

P value	In words	Symbol
≤ 0,001	Extremely significant	***
0,001 – 0,01	Highly significant	**
0,01 – 0,05	Significant	*
> 0,05	Not significant	ns

4 Results

4.1 Characterization of the co-culture system

In-vitro models of the peripheral sensory network face two major problems to accurately mimic the *in-vivo* situation: First, the peripheral terminals of the sensory neurons have to be spatially separated from their cell bodies in the dorsal root ganglia. Second, non-neuronal cells in the periphery require completely different microenvironments and thus, different cultivation conditions. To address questions about the growth dependency of the peripheral axonal fibers in the skin, current mixed culture models of DRGs and skin cells [94] are not sufficient.

Here, a more accurate co-culture model was developed that allows the cultivation of neuronal somata and their axonal processes in separate compartments. A silicon seal allows for different cultivation conditions in the middle and side compartments while remaining penetrable for axonal processes. **Figure 9 B)** shows a schematic draft of a co-culture chamber with one middle and two side compartments.

Figure 9 C) shows a section of a representative co-culture chamber at day 10 stained with anti-pan axonal neurofilament marker SMI312 and DAPI. Dissociated dorsal root ganglion cells were seeded into the middle compartment in neuron specific medium and adhered over night. Subsequent loading of the side compartments with the respective growth cues, either NGFβ or skin cells, stated time point d = 0. Total cultivation period comprised 10 days. The length of a single axonal process varied between several μm and up to one cm at day 10. Total neurite outgrowth in the side compartment is quantified as Cumulative Peripheral Neurite Length, CPNL and given in μm.
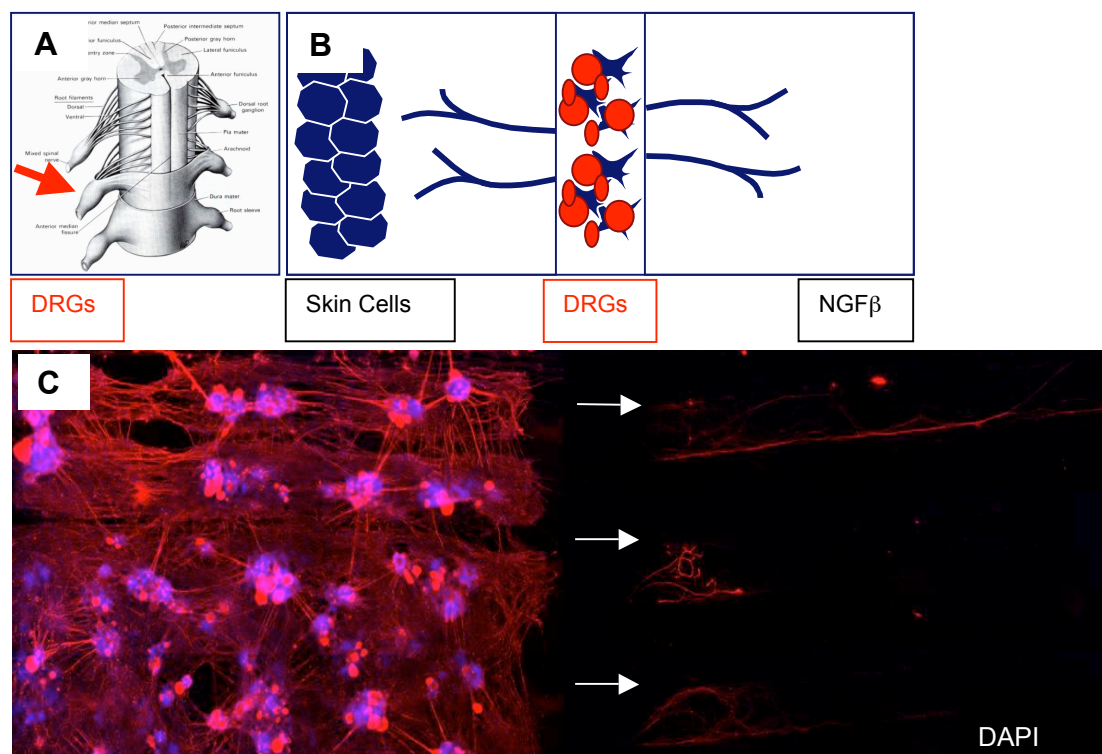
Figure 9: The co-culture system
A) Anatomical illustration of dorsal root ganglia lateral to the spinal cord
(www.laesieworks.com)
B) The co-culture chamber: DRGs are seeded into the middle compartment; NGFβ or
skin cells are loaded into the side compartments as growth cue. Neurites grow through
the silicon sealed borders.
C) Immunofluorescent picture of a representative co-culture chamber (middle and side
compartment) at day 10. Growth cue: 10 ng/mL huNGFβ. DRGs and peripheral
processes were labeled with mouse monoclonal anti-SMI312, goat anti-mouse Alexa
Fluor 594 and DAPI. Arrows indicate the position of axonal processes in the side
compartment. The picture was taken as a mosaic of 52 images at 100x magnification
with an Axiovert S100 microscope (Zeiss).

4.1.1 Effect of NGFβ on neuronal fiber growth

The sensitivity of the co-culture system was investigated using nerve growth factor
(NGF). NGF is a potent neurotrophic factor and known to induce neuronal growth and
differentiation. The neurotrophic effects of NGF are mediated by its β subunit [73].

Therefore, recombinant human NGFβ (Sigma) was used to assess NGF induced fiber
growth in the present co-culture system. Increasing concentrations of huNGFβ (0,04
ng/mL, 0,02 ng/mL, 1 ng/mL, 5 ng/mL and 10 ng/mL) were loaded into the side
compartment of the co-culture chambers. Medium served as negative control and

cumulative peripheral neurite growth (CPNL) in the side compartments was monitored and analyzed at days 4, 5, 6 and 10.

Figure 10 A) shows the increase in CPNL with time. The main increase in growth occurrs between day 6 and 10 and 10 ng/mL huNGFβ exhibits the greatest growth promoting effect. In **B)** the cumulative peripheral fiber growth at day 10 caused by each concentration of huNGFβ is displayed, a detailed representation of the boxed section in **A)**. Data were analyzed for non-linear regression, resulting in a sigmoidal dose-response curve **C)** with an R^2 of 0,9750. The half maximal effective concentration (EC_{50}) determined is 4,524 ng/mL.

These results indicate that NGFβ mediates neurite outgrowth in a dose dependent manner. No outgrowth is caused by medium without stimulus and is therefore run as negative control in all further experiments. 10 ng/mL huNGFβ exhibits the greatest outgrowth promoting effect, already in the range of saturation according to the sigmoidal dose-response curve in C). 10 ng/mL huNGFβ is therefore used as positive control in further experiments.
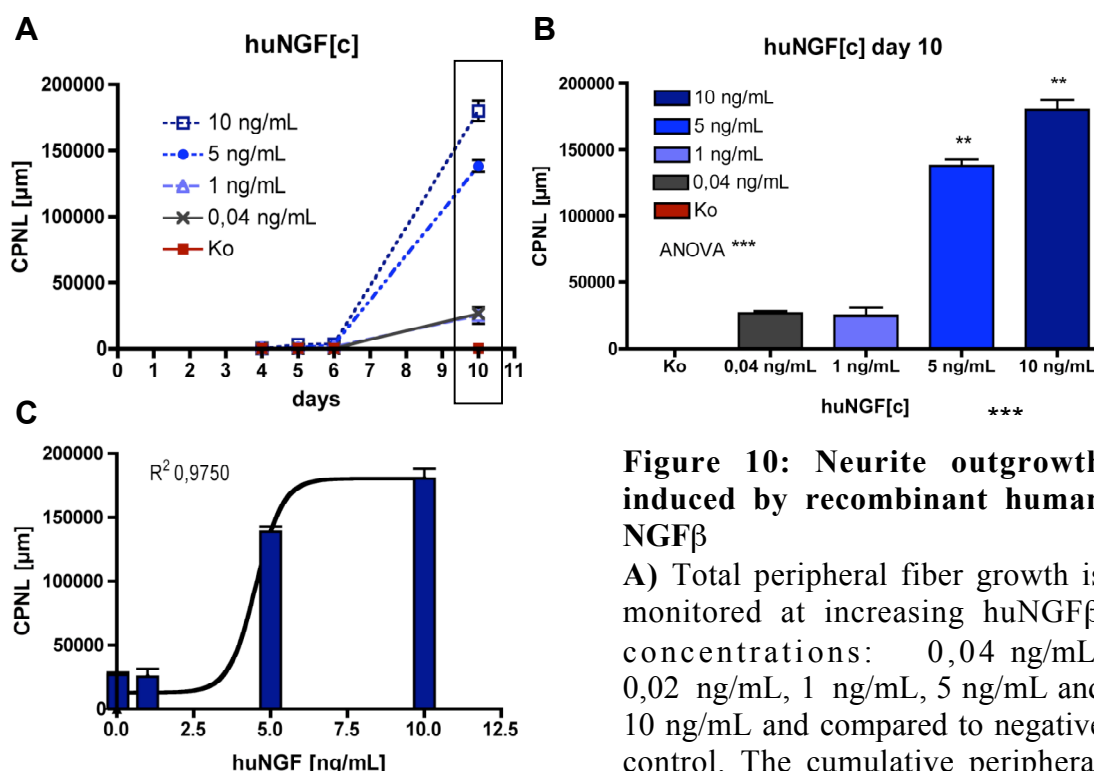
A

huNGF[c]

B

huNGF[c] day 10

C

Figure 10: Neurite outgrowth induced by recombinant human NGFβ

A) Total peripheral fiber growth is monitored at increasing huNGFβ concentrations: 0,04 ng/mL, 0,02 ng/mL, 1 ng/mL, 5 ng/mL and 10 ng/mL and compared to negative control. The cumulative peripheral neurite length (CPNL) was detected at days 4, 5, 6 and 10.

B) Cumulative peripheral neurite length at day 10 at increasing concentrations of huNGFβ. Differences between overall means were analyzed by one-way ANOVA ($^{***}P \leq 0,001$) followed by Dunnett's multiple comparisons test to compare all columns vs. control ($^{**}P$ 0,001 – 0,01). **C)** Data as in B) analyzed for non-linear regression. Plotted is a sigmoid dose-response curve (R^2 0,9750), EC_{50} equals 4,524 ng/mL. (n = 3, run in duplicates)

Additionally, an anti-NGFβ antibody (affinity purified, R&D) was applied to selectively neutralize the growth effects mediated by huNGFβ. The capacity of the anti-NGFβ antibody to neutralize the biological activity of NGFβ was previously shown in an ^{3}H-thymidine incorporation assay with TF-1 cells [91]. Here, two types of experiments were conducted:

First, the capability of the antibody to block NGFβ mediated fiber growth in the co-culture system was investigated. 10 ng/mL huNGFβ and 2μg/mL antibody were applied simultaneously in the side compartment and cumulative peripheral neurite growth was detected.

Figure 11 A) shows the fraction of remaining fiber growth (%) in the presence of the anti-NGFβ antibody compared to the positive control 10 ng/mL huNGFβ (100 %). Fiber growth is reduced to ***3,5 ±4,5 %. The ability of the anti-NGFβ antibody to

neutralize peripheral fiber growth in the co-culture system is considered highly significant.

Second, it is tested whether the successful sequestration of NGF could be controlled by detecting unsequestered, free NGF with the Bioplex Cytokine Assay (Bio-Rad). A complexation assay was conducted. 10 ng/mL huNGFβ were mixed with increasing concentrations of anti-NGFβ antibody. 10 ng/mL huNGFβ without antibody served as positive control. Following 15 min incubation at RT the remaining amount of free NGFβ in solution was detected.

In **Figure 11 B)** the free amount of huNGFβ in solution (pg/mL) is depicted at increasing concentrations of anti-NGFβ antibody: 0,01 µg/mL, 0,05 µg/mL, 0,1 µg/mL, 1 µg/mL and 2 µg/mL. A significant reduction of free NGFβ is achieved with [*]0,10 µg/mL, [**]1 µg/mL and [**]2 µg/mL antibody.
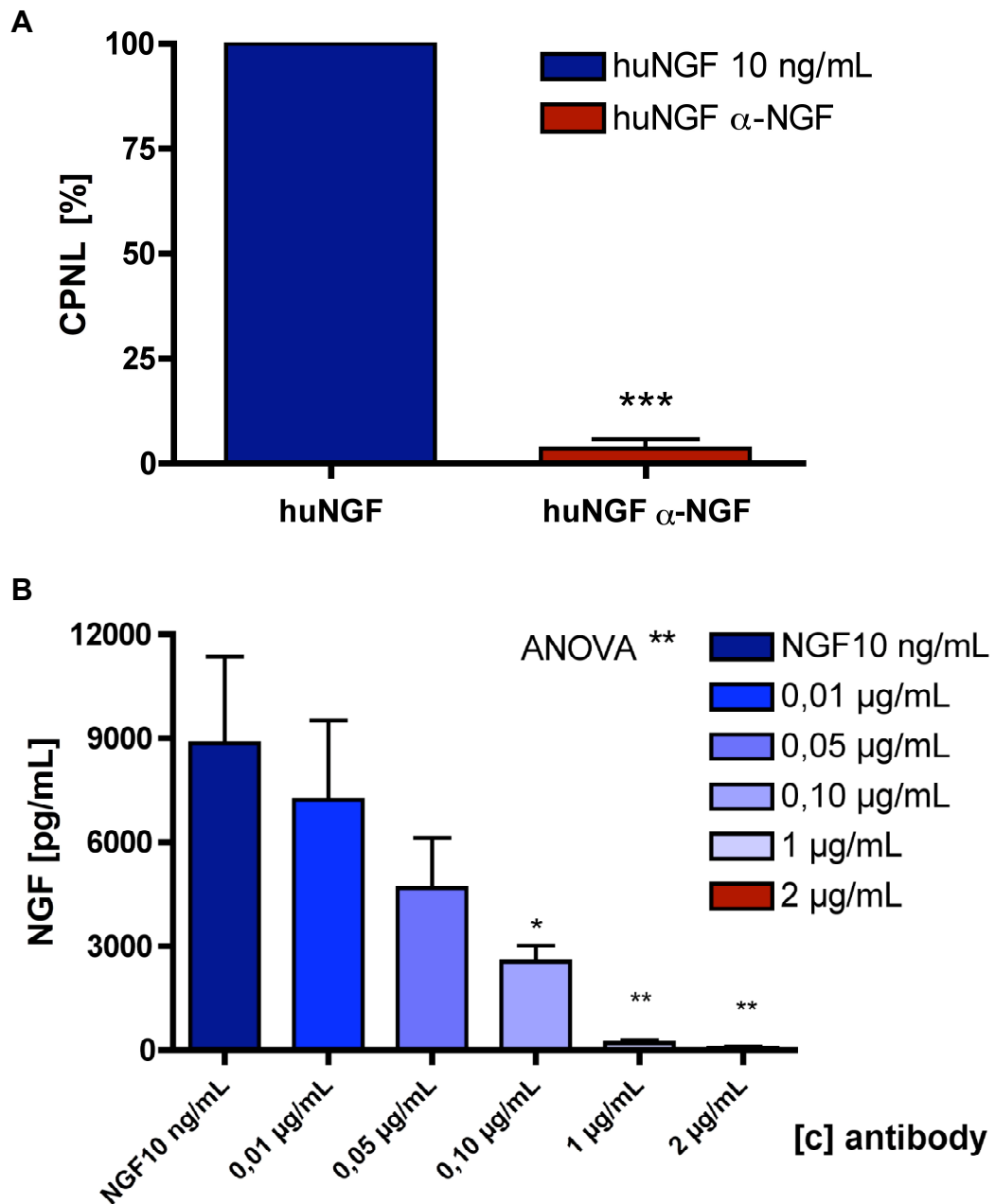
Figure 11: Analysis of neutralization capacity of anti-NGFβ antibody
A) Effect of NGF sequestration with anti-NGFβ antibody (2 ng/mL) on NGFβ (10 ng/mL) induced peripheral fiber growth. The graph shows the percent (%) of fiber growth in the presence of the antibody compared to the positive control. Columns were compared by t-test ([***]P ±0,001). (n = 4, run in duplicates)
B) Sequestration of 10 ng/mL huNGFβ with increasing concentrations of anti-NGFβ antibody: 0,01 µg/mL, 0,05 µg/mL, 0,10 µg/mL, 1 µg/mL and 2 µg/mL. Free NGFβ was detected by Bioplex Cytokine assay. Differences between overall means were compared by one-way ANOVA ([**]P 0,01 – 0,05). Individual means were compared to control by Dunnett's multiple comparisons test ([**]P 0,001 – 0,01; [*]P 0,01 – 0,05). (n = 2, run in duplicates)

4.1.2 Characterization of nociceptive DRGs and fibers via IF staining

In general, dorsal root ganglion cells are classified by the expression of several neurotransmitters, surface receptors, as well as their binding properties for the plant lectin IB4 and their neurotrophic dependency on either NGF or glial cell derived neurotrophic factor GDNF [34]. Dissociated dorsal root ganglion cells of several species have previously been stained for the expression of these markers [28]. However, reliable quantitative studies of their expression pattern in the peripheral target tissues, as the skin, remain elusive.

The co-culture system provides the possibility to analyze the expression of sensory neuronal markers at the peripheral axonal fibers grown in different environments. Here the nociceptive expression pattern of fibers grown in the presence of 10 ng/mL huNGβ in the side compartment was investigated via immunofluorescence staining.

At day 10 cells were fixed with 4 % paraformaldehyde (PFA). Somata and peripheral fibers were labeled for the nociceptive, peptidergic markers calcitonin-gene-related-peptide (CGRP) and the receptor tyrosine kinase TrkA, the non-peptidergic marker Isolectin B4 (IB4) and the vanilloid receptor TRPV1. Total peripheral fibers were labeled with the pan axonal markers SMI312 and PGP9.5, respectively. Cell nuclei were stained with DAPI.

Figure 12 A) shows representative pictures of DRG somata and peripheral neurites. CGRP, TrkA, IB4 and TRPV1 are labeled.in green (Alexa 488) and total peripheral fibers in red (Alexa 594). All four markers are detected to varying extent on somata and fibers. CGRP, TrkA and IB4 are observed alongside the axonal shafts, whereas TRPV1 is present at axonal terminals.

B) The graph depicts the quantification of peripheral marker expression. The fraction (%) of peripheral fiber length labeled for each marker is compared to cumulative fiber length (100 %, grey dotted line). TRPV1 is expressed by approximately 4,6 %, TrkA by 17,8 %, CGRP by 54,7 % and IB4 by 63,8 % of cumulative peripheral fibers.

C) The table summarizes the relative expression (%), standard deviations (SD and SEM) and number of experiments per marker (n).
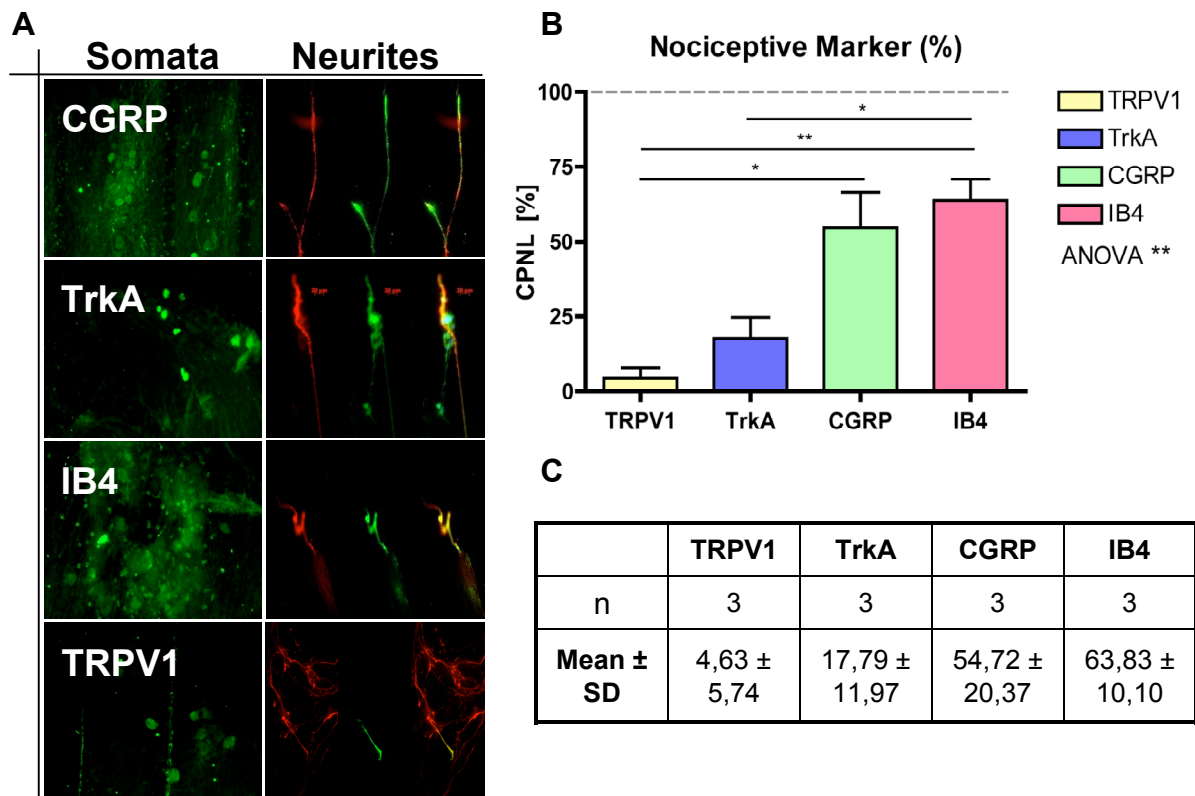
Figure 12: Nociceptive expression pattern of NGFβ induced peripheral fibers
Neurite outgrowth was induced by 10 ng/mL huNGFβ. DRGs were fixed at day 10 with 4 % PFA and stained for the nociceptive, peptidergic markers calcitonin-gene-related-peptide (CGRP) and the receptor tyrosine kinase TrkA, the non-peptidergic marker Isolectin B4 (IB4) and the vanilloid receptor TRPV1 (Mouse monoclonal anti-CGRP, rabbit polyclonal anti-TrkA, rabbit polyclonal anti-TRPV1, Isolectin GS-IB4 Alexa Fluor 488 conjugate). Total peripheral fibers were labeled with either mouse monoclonal anti-SMI312 or rabbit polyclonal anti-PGP9.5. (CPNL, cumulative peripheral neurite length)
A) Immunofluorescent staining of DRG somata and respective peripheral neurites. CGRP, TrkA, IB4 and TRPV1 were stained in green with Alexa 488 (Goat anti-mouse Alexa Fluor 488, goat anti-rabbit Alexa Fluor 488, Isolectin GS-IB4 Alexa Fluor 488 conjugate). Total peripheral fibers were labeled in red with Alexa 594 (Goat anti-mouse Alexa Fluor 594, goat anti-rabbit Alexa Fluor 594).
B) Expression pattern of CGRP, TrkA, IB4 and TRPV1: Plotted is the fraction (%) of peripheral fiber length expressing each marker compared to total fiber length (100 %). Differences between overall means were analyzed by one-way ANOVA (**P 0,001 – 0,01). Individual columns were compared by Bonferroni's multiple comparisons post-test (**P 0,001 – 0,01; *P 0,01 – 0,05).
C) Table indicating average total length (%) ± standard deviation for each marker expressed in the peripheral fibers (n=3; experiments run in duplicates)

4.1.3 Stimulation of DRGs and peripheral fibers

It was investigated whether cultured DRGs and their peripheral fibers are functional and therefore can be stimulated to release the neurotransmitter CGRP, an efferent function of DRGs. To examine further, whether stimulation of DRGs in the middle compartment is relayed to axonal terminals in the side compartment, application of stimuli was confined to the middel chamber. Unspecific stimulation was performed with high potassium at a concentration of 50 mM **(Figure 13)**. Specific, receptor dependent stimulation was conducted with 50 nM capsaicin (CPS) that exerts its function by binding to the receptor TRPV1. The specific inhibition of capsaicin mediated stimulation was examined with the synthetic TRPV1 antagonist capsazepine (CPZ), added in a 10-fold excess over CPS at 500 nM **(Figure 14)**.

DRGs were cultivated with 10 ng/mL huNGFβ in the side compartment and subjected to stimulation experiments at day 10. Each stimulation cycle comprised of a wash step, 10 min incubation with HEPES buffer to determine basal CGRP release, followed by 10 min incubation with the stimulus applied to the middle compartment. After each 10 min incubation period the supernatants of middle and side compartments were collected. The concentration of CGRP was detected by EIA (Cayman).

Figure 13 depicts the results for stimulation with high potassium. In **A)** the CGRP content of the middle compartment is plotted for two consecutive stimulation cycles. Basal CGRP release of 60,3 ±43,2 and 72,8 ±17,89 pg/mL after the first and second HEPES incubation is detected. Following the stimulation with high potassium, CGRP concentration is increased to *344,2 ±145,0 pg/mL (*P <0,05) in the first cycle and to **184,4 ±19,7 pg/mL (**P 0,001 – 0,01) in the second cycle. In **B)** the CGRP content of the side compartment is plotted for two consecutive stimulation cylces. A basal release of 5,2 ±7,3 pg/mL and 31,8 ±44,5 pg/mL CGRP in the first and second cycle is detected. Following the application of high potassium to the middle compartment, the CGRP content in the side compartment is increased to **105,4 ±4,2 pg/mL (**P 0,001 – 0,01) for the first cycle and 84,0 ±2,4 pg/mL for the second cycle. During the second HEPES application, CGRP release does not completely return to the basal level. Hence, the second basal and induced release of CGRP are not significantly different. However, the second stimulation is highly significant compared to the initial basal level during HEPES application in the first cycle.

Figure 13 C) shows two representative pictures of immunofluorescent labeled neuronal fibers before (-K$^+$) and after stimulation (+K$^+$). Total peripheral fibers are labeled with a primary anti-PGP9.5 antibody and stained red with Alexa 594. CGRP is stained green with a primary anti-CGRP antibody and Alexa 488. Following two cycles of stimulation the CGRP content of the fibers is clearly reduced.

Hence, the stimulation with high potassium (50 mM) is used as positive control in all subsequent stimulation experiments.
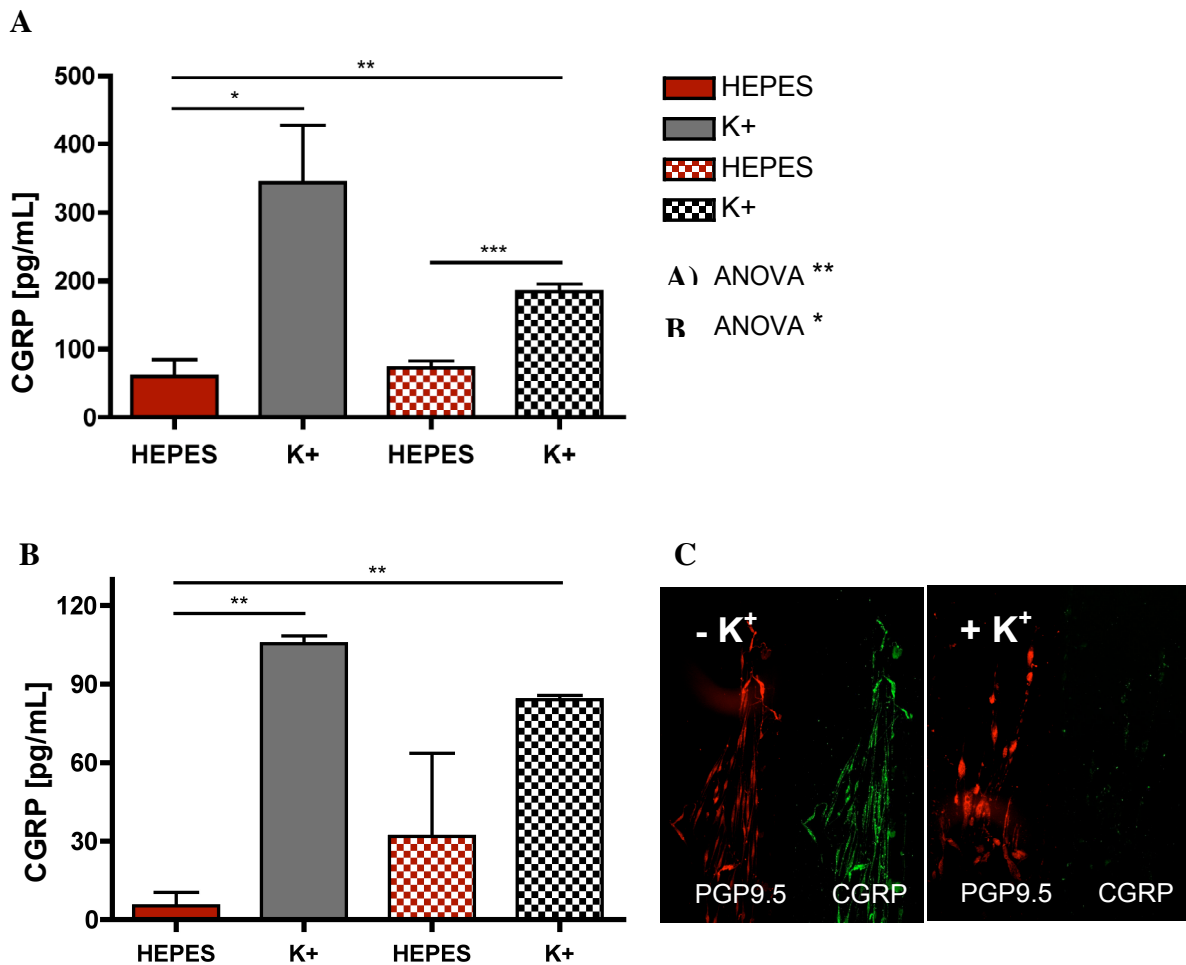
Figure 13: Stimulation of CGRP release with potassium

Repetitive stimulation of DRGs with 50 mM potassium at day 10; Neurite outgrowth was induced by 10 ng/mL huNGFβ. Supernatants of middle and side compartments were subjected to EIA for quantification of CGRP. Basal CGRP release was detected in HEPES without stimulus.

A) Middle compartment: CGRP concentration (pg/mL) in the supernatants of two consecutive stimulation cycles. Differences between overall means were analyzed by one-way ANOVA (**P 0,001 – 0,01). Individual means were compared by Bonferroni's multiple comparisons post-test (*P 0,01 – 0,05) and t-test (***P <0,001; **P 0,001 – 0,01). (n = 3, total of 14 middle chambers out of 3 piglets)

B) Side compartment: CGRP concentration (pg/mL) in the supernatant of two consecutive stimulation cycles. Differences between overall means were analyzed by one-way ANOVA (*P 0,01 – 0,05). Individual means were compared by t-test (**P 0,001 – 0,01). (n = 3, run in duplicates)

C) Representative pictures of immunofluorescent staining; CGRP in green and PGP9.5 in red (Mouse monoclonal anti-CGRP, rabbit polyclonal anti-PGP9.5, goat anti-mouse Alexa 488, goat anti-rabbit Alexa 594) chamber fixed and stained before stimulation (–K^{+}) and chamber fixed and stained after two cycles of stimulation (+K^{+}). Pictures were taken at 100x magnification with an Axiovert S100 microscope (Zeiss).

Figure 14 shows the CGRP release induced by stimulation with capsaicin (CPS) and the specific block of CPS stimulation with capsazepine (CPZ) in **A)**, as well as the persistent unspecific stimulation with high potassium in the presence of CPZ in **B)**. The first cycle of stimulation is displayed. Detected CGRP concentration is normalized to cumulative peripheral fiber growth (pg/(mL**.**μm) to minimize errors derived from unequal fiber outgrowth.

In **A)** the stimulation with 50 nM CPS is compared with co-application of CPS and 500 nM CPZ (1:10). CPS elevates the CGRP concentration 2,3 fold compared to its basal level after HEPES incubation (p 0,0607). On the other hand, co-application of CPS and CPZ does not increase the CGRP concentration compared to the basal level. Notably, the CGRP concentration after CPS stimulation compared to the co-application of CPS:CPZ exhibits a [*]4 fold ([*]P <0,05) decrease.

In **B)** the simultanous application of 50 mM potassium and 500 nM CPZ is indicated. The CGRP concentration in the side compartment is increased [*]2,2-fold ([*]P <0,05) compared to the basal level.

In summary, stimulation of DRGs with the TRPV1 agonist CPS is specifically blocked by its antagonist, whereas unspecific stimulation with potassium is not.
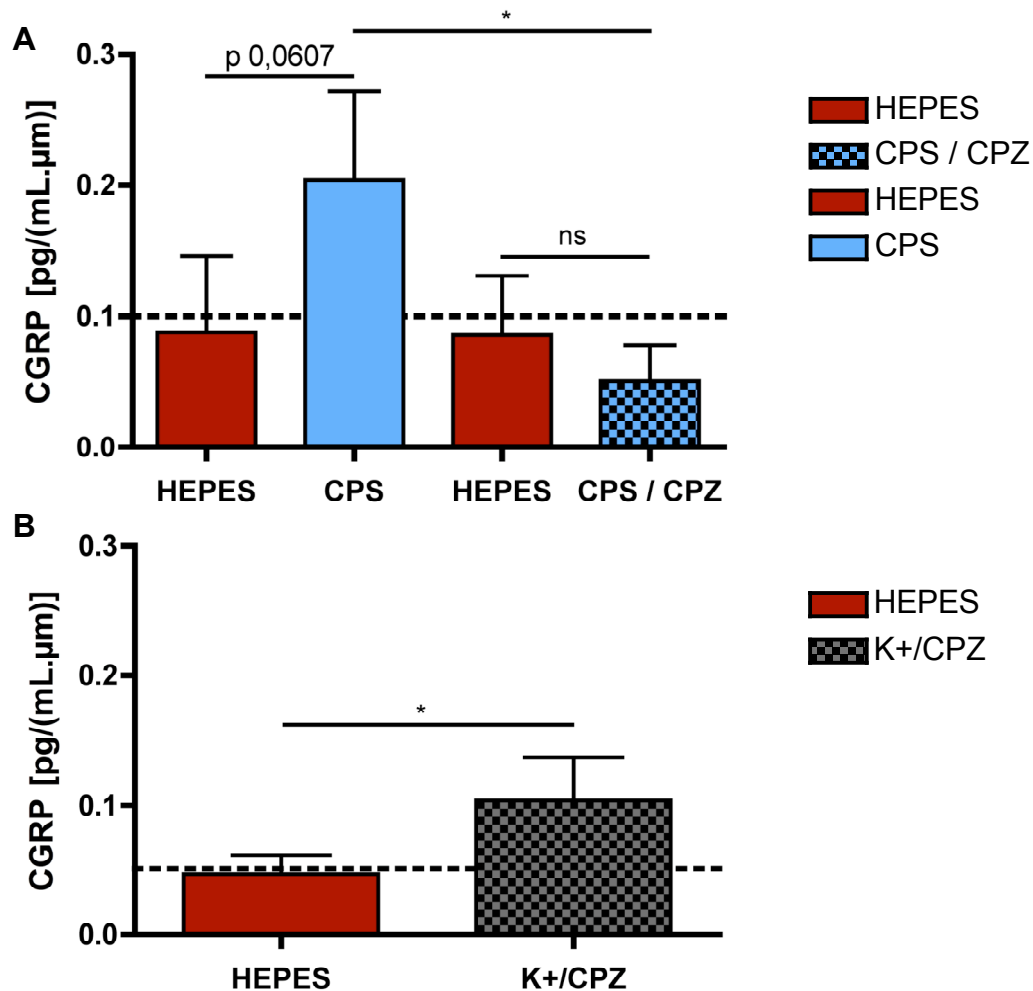
Figure 14: Stimulation of DRGs with the TRPV1 agonist capsaicin (CPS) and antagonist capsazepine (CPZ)

Stimulation at day 10 of neurite outgrowth induced by 10 ng/mL huNGFβ. Concentration of CGRP (pg/mL) in the supernatant was normalized to cumulative peripheral neurite growth (CPNL in µm) of the respective side compartment. Basal CGRP release was detected in HEPES without stimulus.

A) Stimulation with 50 nM CPS and co-application of 50 nM CPS and 500 nM CPZ (1:10). Plotted is the CGRP content of the supernatant in the side compartment normalized with total fiber growth (pg/(mL.µm)). Differences between individual means were compared by t-test (*P 0,01 − 0,05). (CPS/CPZ n = 3; CPS n=4, run in duplicates)

B) Co-application of 50 mM potassium (K^+) and 500 nM CPZ: Plotted is the CGRP content of the supernatant in the side compartment normalized with total fiber growth (pg/(mL.µm)). Differences between means were compared by t-test (*P 0,01 − 0,05). (n = 3, run in duplicates)

4.2   NGF expression and secretion by human skin cells

The ability of skin cells to produce and secrete NGFβ has previously been shown by different groups [100] [101] [102]. In order to address questions about the growth effects of peripheral axonal fibers mediated by skin cells, the expression and secretion pattern of NGFβ by keratinocytes and fibroblasts were determined. In addition, the content of NGFβ in the supernatants of co-cultures with skin cells was detected.

4.2.1   Kinetics of NGFβ expression and secretion

Keratinocytes and fibroblasts were cultivated for 10 days in mono-culture, in an equal cells per cm^2 to volume ratio as in co-culture side compartments. The concentration of NGFβ in the supernatants of skin cells was detected at day 2, 4, 6, 8 and 10 using the Bio-Plex Cytokine Assay. In parallel, the total protein concentration of cell lysates was determined with the BCA Protein Quantification Kit. Detected concentrations of NGFβ were normalized to respective total protein concentrations.

In a second parallel setup skin cells were lysed and subjected to mRNA isolation at day 2, 4, 6, 8 and 10. Following reverse transcription the expression levels of NGFβ were detected by real time PCR using the TaqMan human NGFβ Gene Expression Assay (Applied Biosystems). Detected Expression levels of huNGFβ were normalized using the endogenous control 18S rRNA.

Figure 15 summarizes the kinetics of NGFβ expression and secretion by primary skin cells over 10 days in culture. NGFβ mRNA and protein is detectable in both, keratinocytes as well as in fibroblasts. In **A)** ddCt values of NGFβ expression of keratinocytes and fibroblasts are plotted with cultivation time. Fibroblasts show significantly higher expression levels compared to keratinocytes at all time points.

This tendency is also reflected in the protein levels shown in **B)**. The normalized concentration of NGFβ in the supernatants of skin cells per mg total protein (pg/mg) is plotted with cultivation time. The concentration of NGFβ in the supernatants of fibroblasts is several folds higher compared to keratinocytes at all time points. Furthermore, a significant effect on NGFβ levels by days is detected. NGFβ concentration in the supernatant increases for both cell types with a peak at day 6, followed by a decrease of levels at day 8 and 10.
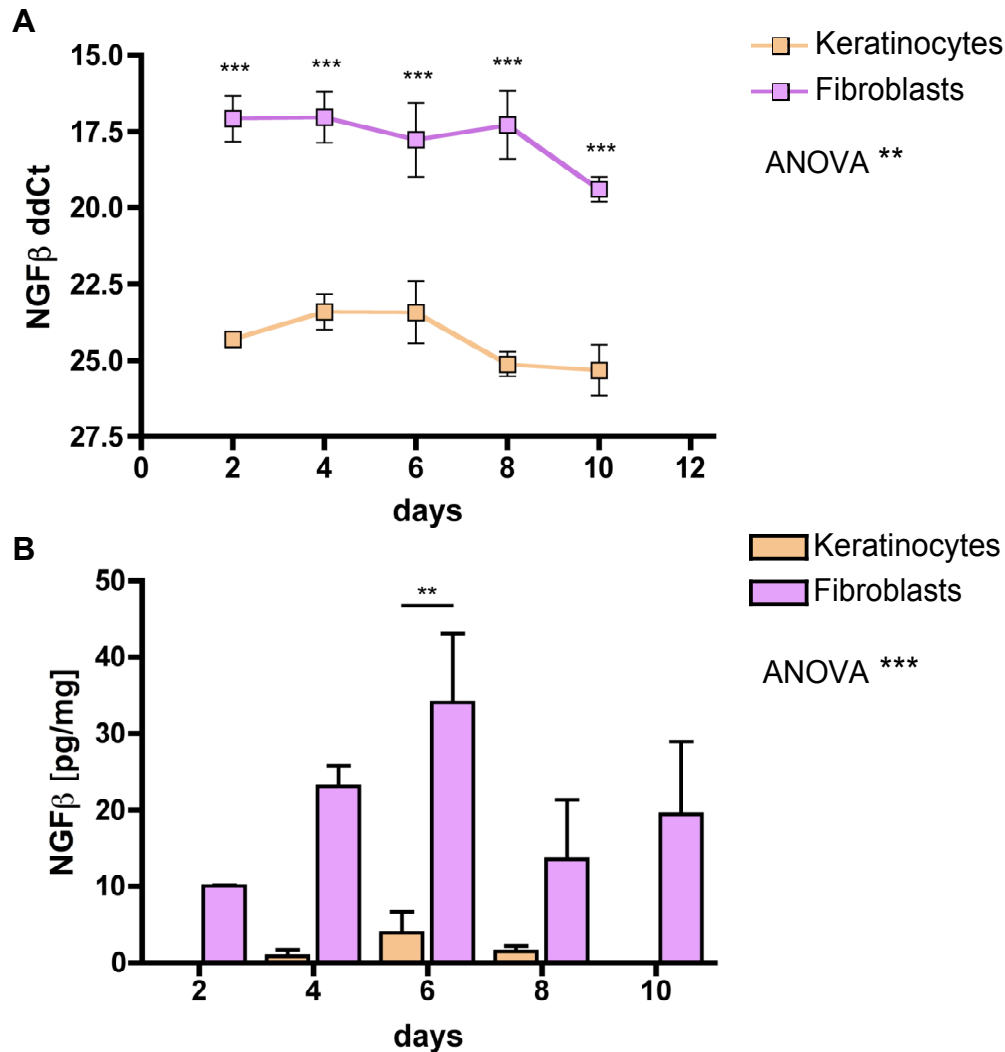
Figure 15: NGFβ expression and secretion by primary skin cells
Keratinocytes and fibroblasts were cultivated for 2, 4, 6, 8 and 10 days. Cells / cm^2 to volume ratio as in the co-culture side compartments. Two parallel setups were conducted: **i)** NGFβ in the supernatants was quantified and normalized to total protein concentration. **ii)** mRNA was isolated, transcribed to cDNA and subjected to real time PCR for the detection of NGFβ expression levels. (n = 2, run in duplicates)
A) Expression levels of NGFβ (ddCt values) in keratinocytes and fibroblasts at day 2, 4, 6, 8 and 10. Expression levels were normalized to the endogenous control 18S rRNA. Overall expression of NGFβ in keratinocytes and fibroblasts was compared by two-way ANOVA (**P 0,001 – 0,01). Values of individual time points were compared by Bonferroni's post-test (***P ±0,001).
B) Normalized concentrations of NGFβ (pg/mg total protein) in the supernatants of keratinocytes and fibroblasts at day 2, 4, 6, 8 and 10. Overall NGFβ concentrations in the supernatants of keratinocytes and fibroblasts were compared by two-way ANOVA (***P ±0,001). Values of individual time points were compared by Bonferroni's post-test (**P 0,001 – 0,01).

4.2.2 NGFβ concentration of co-culture supernatants

The content of NGFβ in the supernatants of primary skin cells co-cultivated in co-culture chambers over 10 days was determined. Cells were seeded in the side compartments at day 0. Supernatants were subjected to Bio-Plex Cytokine Assay for NGFβ detection every second day before replacement of the medium.

Figure 16 shows the average concentration of NGFβ in the supernatants of keratinocytes and fibroblasts in co-culture chambers. Each data set comprises five values representing the NGFβ concentration at day 2, 4, 6, 8 and 10. Each individual value is an average of 6 (keratinocytes) and 4 (fibroblasts) experiments, ran in duplicates. NGFβ concentrations detected are within the same range as previously defined in 4.2.1. However, no difference of NGFβ levels between keratinocytes and fibroblasts is observed.
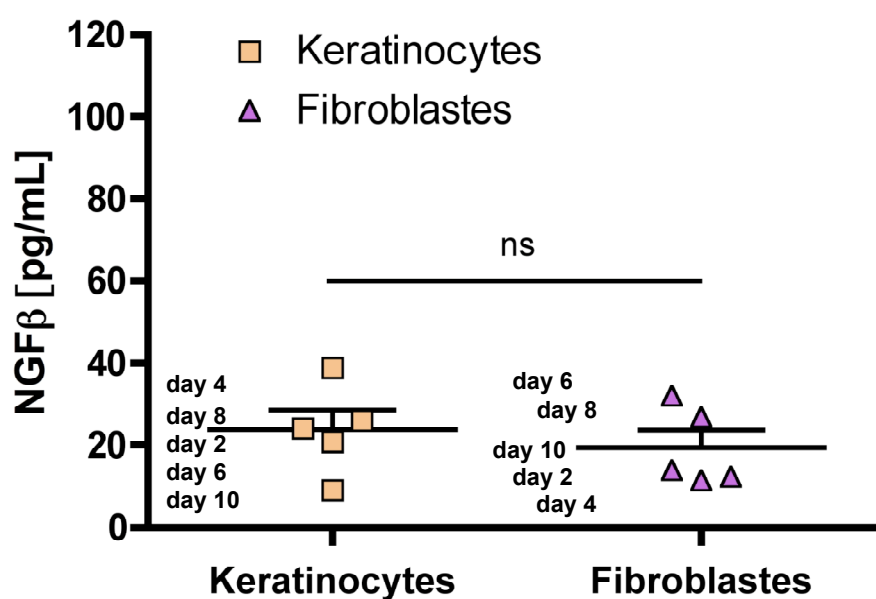

Figure 16: Concentration of NGFβ in supernatants of skin cells in co-culture chambers
Keratinocytes and fibroblasts were seeded into the side compartment of co-culture chambers and cultivated for 10 days. NGFβ detection in the supernatants of skin cells every second day before media replacement.
The graph shows five values representing NGFβ concentrations (pg/mL) at day 2, 4, 6, 8 and 10 of keratinocyte and fibroblast supernatants, respectively. (Keratinocytes n = 6; Fibroblasts n = 4, run in duplicates)

4.3 Effect of primary skin cells on peripheral fiber growth

Peripheral neurite growth in the side compartment of co-culture chambers is induced by huNGFβ in a dose dependent manner. Furthermore, keratinocytes and fibroblasts express and secrete huNGFβ. In the present co-culture system, it was investigated whether primary skin cells serve as sufficient growth cue to induce peripheral neurite growth.

In a second step, it was examined whether endogenously produced NGFβ is necessary for peripheral neurite growth mediated by skin cells. Does NGFβ independent outgrowth occur in the presence of keratinocytes and fibroblasts, respectively? An anti-NGFβ antibody (4.1.1) was employed to specifically neutralize growth effects mediated by secreted NGFβ.

Finally, it was analyzed whether NGFβ independent growth occurs due to a soluble factor released into the supernatants and therefore can be mimicked by conditioned media of skin cells.

4.3.1 Peripheral fiber growth mediated by primary skin cells

Keratinocytes and Fibroblasts were seeded into the side compartment of co-culture chambers and cultivated for 10 days. Respective cultivation media (KGM-2, DMEM, F12) served as negative controls and 10 ng/mL external huNGFβ was used as high standard positive control. Peripheral fiber growth was monitored and analyzed at day 10.

Figure 17 A) shows representative pictures of immunofluorescent labeled skin cells and neurites in co-culture. Total peripheral fibers are labeled in red with anti-pan axonal neurofilament marker SMI312 or anti-PGP9.5, followed by Alexa 594 coupled secondary antibodies. Fibroblasts and keratinocytes are labeled in green with anti-fibroblast surface protein (FSP) and anti-wide spectrum cytokeratin, followed by Alexa 488. Peripheral neurites induced by fibroblasts and keratinocytes differ in their phenotype. Fibers entering the keratinocyte layer grow along the cell borders, branch and wrap around individual keratinocytes (arrows). Fibroblast induced neurites exhibit minor branching and wrapping. **B)** shows the quantification of neurite outgrowth mediated by skin cells compared to control and high standard 10 ng/mL huNGFβ. Both fibroblasts and keratinocytes are sufficient to induce significant neurite outgrowth compared to medium control, which equaled zero. Surprisingly,

keratinocyte mediated peripheral fiber growth exceeds the values achieved by the high standard 10 ng/mL huNGFβ with 247.899 ±234.649 µm compared to 179.978 ±10.467 μm. The difference is however not significant. Further, fibroblasts mediated 44.882 ±19.486 μm CPNL, which is 4 times less outgrowth compared to 10 ng/mL huNGFβ.
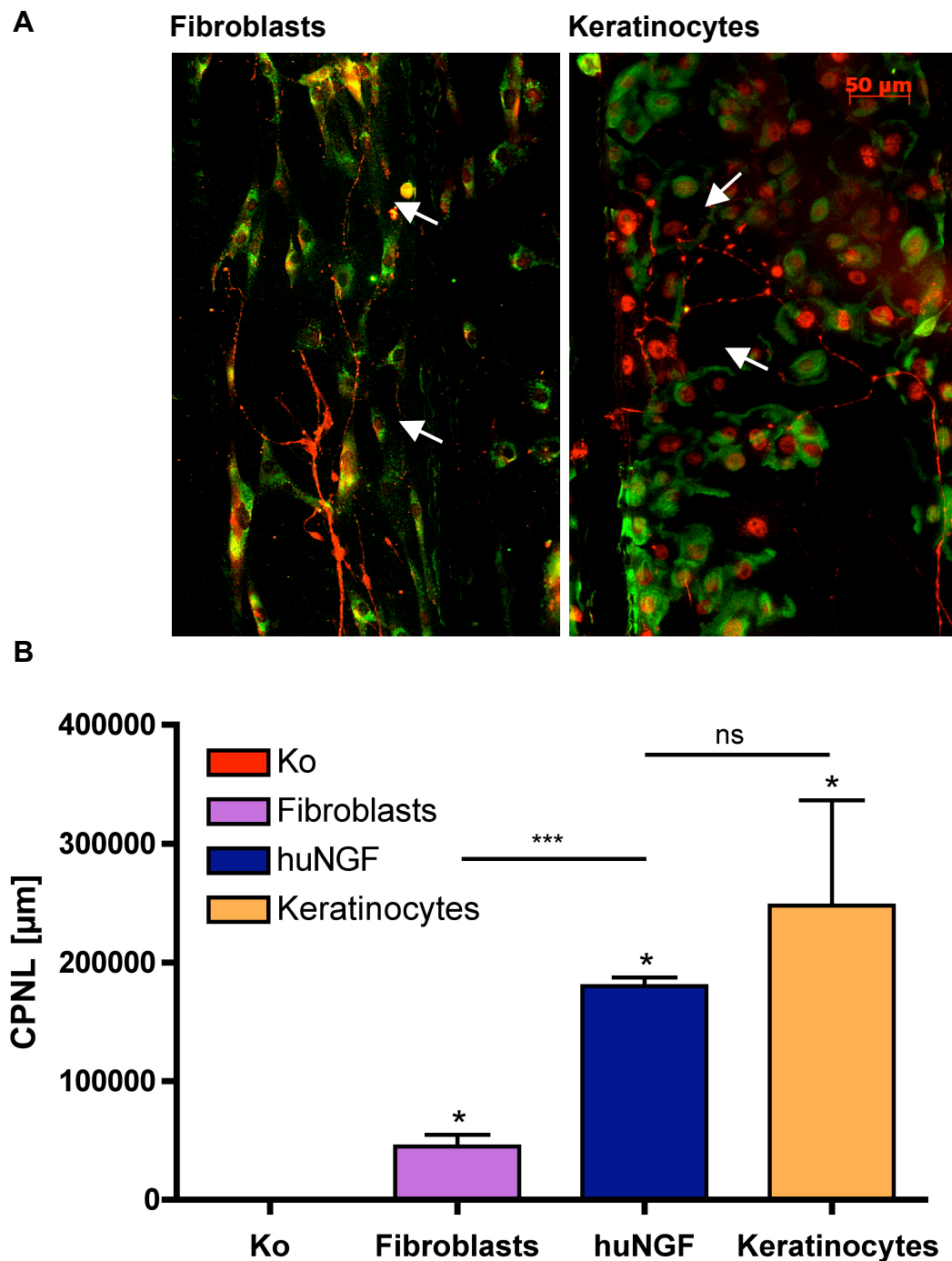
Figure 17: Analysis of neurite outgrowth mediated by skin cells
A) Immunofluorescent stainings of skin cells in co-culture. Fibroblasts and keratinocytes labeled in green with Alexa 488 (mouse monoclonal anti-FSP, polyclonal rabbit anti-wide spectrum cytokeratin; goat anti-mouse Alexa 488, goat anti-rabbit Alexa 488). Neurites labeled in red with Alexa 594 (mouse monoclonal anti-SMI312, rabbit polyclonal anti-PGP9.5; goat anti-mouse Alexa 594, goat anti-rabbit Alexa 594). Pictures were taken as a mosaic at 100x magnification with an Axiovert S100 microscope (Zeiss).
B) Total peripheral fiber growth (µm) at day 10 mediated by: Control (Ko), fibroblasts, 10mL huNGFβ and keratinocytes. Individual means were compared to control via one sample t-test as control equals 0 (*P 0,01 – 0,05). Skin cell mediated fiber growth was compared to huNGFβ mediated growth by t-test (***P ±0,001). (Ko, fibroblasts n = 4; huNGFβ n = 3; Keratinocytes n = 7, run in duplicates)

4.3.2 NGFβ independent fiber growth mediated by primary skin cells

The growth effects mediated by NGFβ secreted by primary skin cells were selectively blocked by an anti-NGFβ antibody. 0,1 µg/mL antibody (approximately 1000-fold excess per epitope in reference to the average concentration measured in co-culture supernatants) was co-applied with keratinocytes and fibroblasts in the side compartments. Fiber growth was monitored and analyzed at day 10.

Figure 18 shows the cumulative peripheral neurite outgrowth mediated by keratinocytes in **A)** and fibroblasts in **B)**. Antibody co-application causes a significant reduction in fiber outgrowth in the presence of both cell types. However, keratinocytes mediate a total of 65.912 ±39.989 µm NGFβ independent outgrowth, compared to 3.451 ±2.308 µm mediated by fibroblasts. Co-application of 10 ng/mL huNGFβ and 2 µg/mL antibody as negative control shows a remaining neurite outgrowth of [***]6.522 ±8.479 µm (4.1.1). Therefore, fibroblast mediated NGFβ independent fiber growth yields CPNLs below control level.
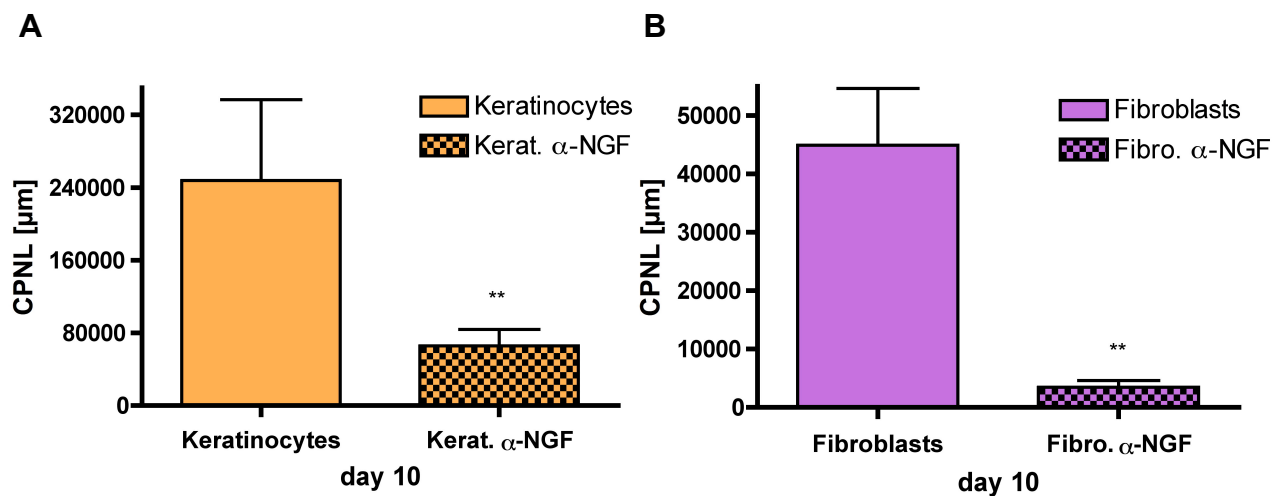

Figure 18: Analysis of NGFβ dependency of peripheral fiber growth mediated by skin cells

A) NGFβ dependency of keratinocyte mediated neurite outgrowth: Cumulative peripheral neurite growth (µm) at day 10 mediated by keratinocytes and keratinocytes plus anti-NGFβ antibody. Means were compared by t-test ([**]P 0,001 − 0,01). (Keratinocytes n = 7; Kerat. anti-NGFβ n = 5, run in duplicates)

B) NGFβ dependency of fibroblast medited neurite outgrowth: Cumulative peripheral neurite growth (µm) at day 10 mediated by fibroblasts and fibroblasts plus anti-NGFβ antibody. Means were compared by t-test ([**]P 0,001 − 0,01). (n = 4; run in duplicates)

4.3.3 Peripheral fiber growth mediated by conditioned media of primary skin cells

As NGFβ is secreted into the supernatant by skin cells (4.2), it was investigated whether conditioned media of keratinocytes and fibroblasts are able to mimic the growth effect of primary skin cells.

Cell culture supernatants of skin cells cultured for two days at >80 % confluence were collected and loaded into co-culture side compartments as growth cue. 0,1 µg/mL anti-NGFβ antibody (approximately 1000-fold excess per epitope in reference to the concentration detected in conditioned media) was pre-incubated with conditioned media at RT for 15min and subsequently loaded into the side compartments. Cumulative peripheral neurite growth was monitored and analyzed at day 10.

Figure 19 shows the cumulative peripheral neurite length mediated by conditioned medium of keratinocytes in **A)** and fibroblasts in **B)**. Conditioned media of both, keratinocytes and fibroblasts mediate fiber outgrowth, with 15.626 ±19.287 µm and 459.367 ±415.853 µm, respectively. Co-application of anti-NGF antibody and conditioned fibroblast medium causes a significant reduction in CPNL of 91,8 %. Co-application of anti-NGF antibody and conditioned keratinocyte medium caused a non significant reduction of 39 % CPNL. Though, absolute values differ from the CPNLs (µm) obtained by skin cells (4.3.2), overall tendency is similar. Different absolute CPNLs may be due to large standard deviations caused by the inconsistency of conditioned media.

In summary, conditioned media mimic the effects of keratinocytes and fibroblasts on fiber growth. Neurite outgrowth mediated by keratinocytes and conditioned keratinocyte medium likely represents an accumulative effect of NGF and at least one additional soluble factor. Fibroblast induced fiber growth is NGF mediated.
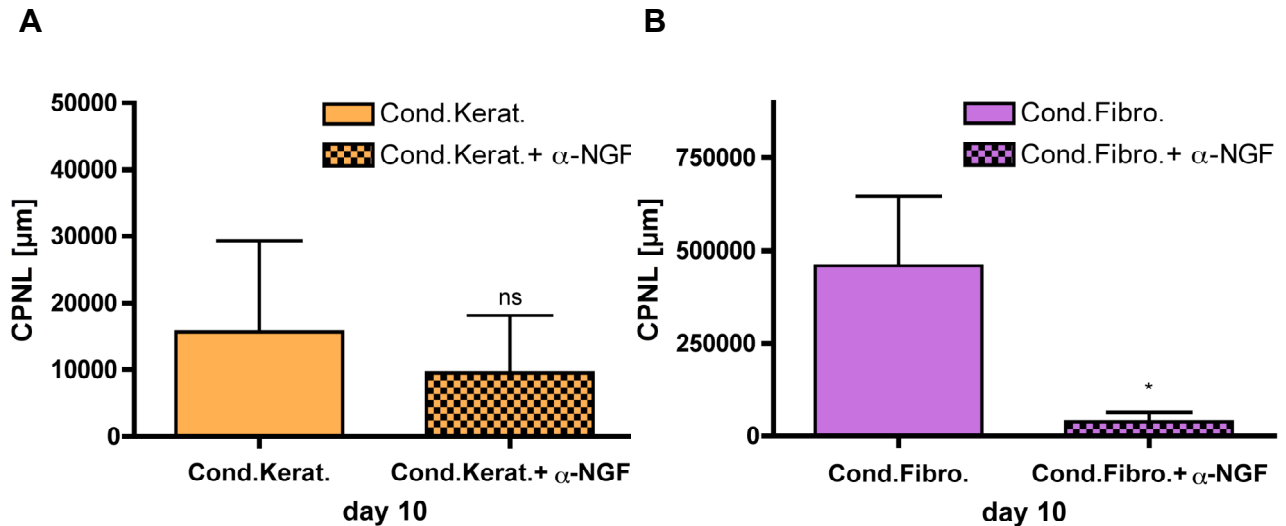
Figure 19: Analysis of NGFβ dependency of peripheral fiber growth mediated by conditioned media of skin cells

A) NGFβ dependency of conditioned media mediated outgrowth, keratinocytes: Cumulative peripheral neurite growth (μm) at day 10 mediated by conditioned keratinocyte medium and co-applied anti-NGFβ antibody. Means were compared by t-test. (n = 2, run in duplicates)

B) NGFβ dependency of conditioned media mediated outgrowth, fibroblasts: Cumulative peripheral neurite growth (μm) at day 10 mediated by conditioned fibroblast medium and co-applied anti-NGFβ antibody. Means were compared by t-test ([*]P 0,01 – 0,05). (n = 5, run in duplicates)

4.4   Quantification of NGFβ independent neurite growth

To quantify and compare NGFβ independent peripheral neurite growth detected in 4.3.2, relative values were calculated for each growth condition.

Skin cells and co-applied anti-NGF antibody were loaded in the two side compartments of the same co-culture chamber. NGFβ independent fiber growth of one side compartment is expressed as percent (%) of total fiber growth present in the second side compartment grown without antibody. Co-application of 10 ng/mL huNGFβ and 2 μg/mL antibody served as negative control.

Figure 20 shows the relative values of NGFβ independent peripheral neurite growth mediated by keratinocytes and fibroblasts compared to controls. No significant difference is detected between negative control and fibroblasts, with 3,53 ±4,54 % and 8,94 ±7,48 % CPNL, respectively. However, keratinocytes mediate significant NGFβ independent outgrowth of [**]42,93 ±25,61 % CPNL ([**]P 0,001 – 0,01). Notably, NGFβ

independent fiber growth induced by keratinocytes is significantly higher compared to fibroblasts.

In summary, approximately 42,9 % of keratinocyte mediated peripheral fibers grow independently of NGFβ and are induced by at least one additional factor. Fibroblasts however induce fiber growth via NGFβ.
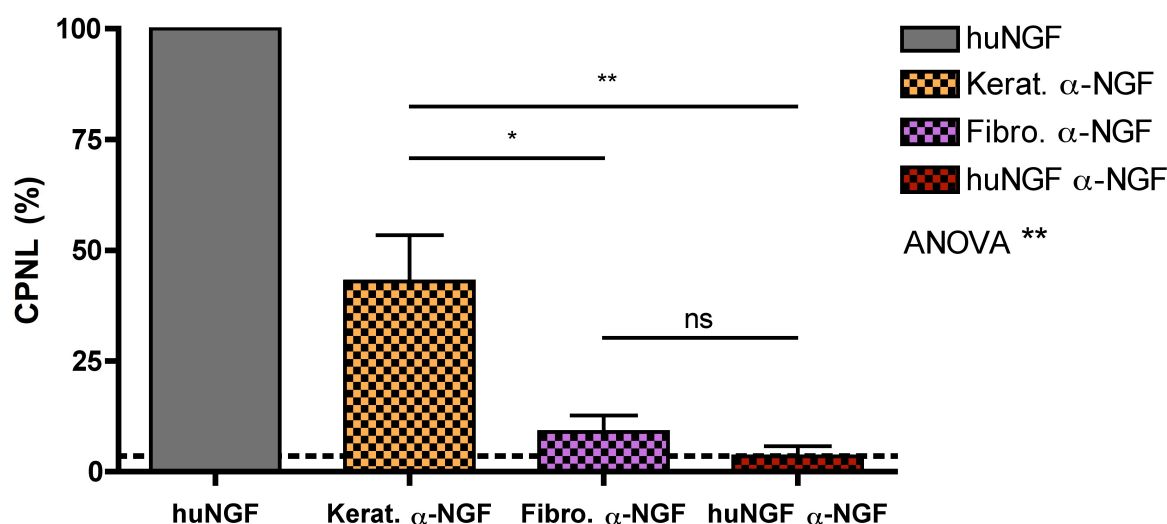

Figure 20: Quantification of NGFβ independent neurite outgrowth
Neurite outgrowth after co-application of primary skin cells and anti-NGFβ antibody was compared and normalized to skin cell mediated growth. NGFβ independent neurite growth is expressed as fraction (%) of cumulative peripheral neurite growth (100 %, grey) of respective control.
Depicted are keratinocytes plus anti-NGF, fibroblasts plus anti-NGF and the negative control 10 ng/mL huNGFβ plus 2 µg/mL antibody.
Differences between overall means were compared by one-way ANOVA ([**]P 0,001 – 0,01). Individual means were compared by Bonferroni's multiple comparisons post-test ([**]P 0,001 – 0,01; [*]P 0,01 – 0,05). (Kerat. anti-NGF n = 6; Fibro. anti-NGF, huNGF anti-NGF n = 4, run in duplicates)

4.5   Kinetics of NGFβ independent fiber growth

As previously shown (4.4), keratinocytes mediate significant NGFβ independent peripheral neurite outgrowth. Here, it was investigated whether neurites mediated by keratinocytes with and without endogenous NGFβ show different kinetics in growth. Co-cultures with keratinocytes only and with co-application of anti-NGFβ antibody were compared. CPNLs in the side compartments were monitored and analyzed at day 4, 6 and 10.

Figure 21 shows cumulative peripheral neurite outgrowth at day 4, 6 and 10 mediated by keratinocytes with and without endogenous NGFβ. The growth curve of both conditions differs significantly. Notably, there is no difference in CPNLs at day 4, with 2.110 ±4.532 μm and 1.450 ±1.661 μm, as well as day 6, with 9.646 ±9.761 μm and 9.404 ±12.216 μm. However, significant difference is detected at day 10, with double the amount of CPNL grown in the presence of endogenously produced NGFβ. Neurites enter the keratinocyte layer approximately at day 6.
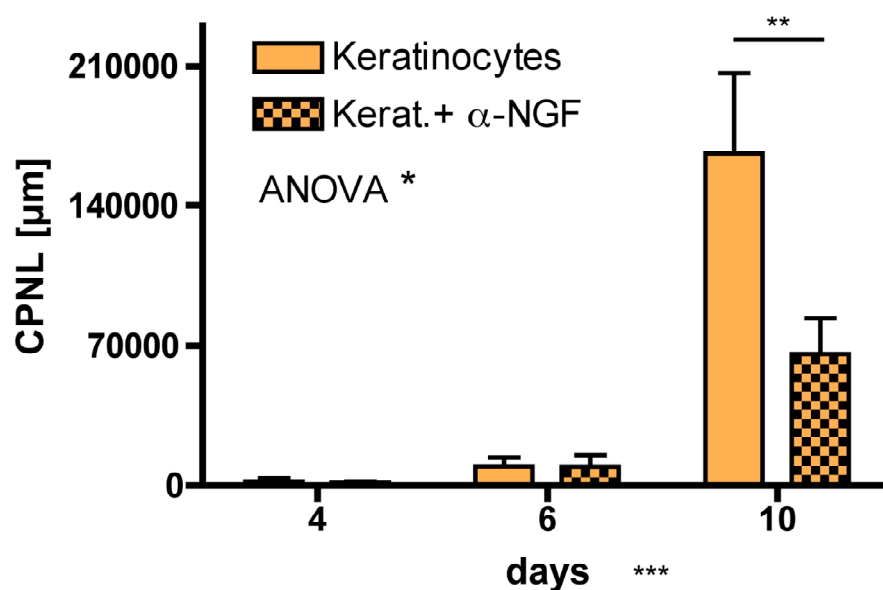
Figure 21: Kinetics of neurite outgrowth mediated by keratinocytes
A) Cumulative peripheral neurite length (μm) at day 4, 6 and 10 of keratinocytes and co-applied anti-NGFβ. Growth kinetics of both conditions (*P 0,01 − 0,05) and increase over days (***P ±0,001) were compared by two-way ANOVA. Cumulative neurite outgrowth of both conditions were compared at day 10 by Bonferroni's post-test (**P 0,01 − 0,05). (n = 6, run in duplicates)

5 Discussion

In the present work the role of NGF in the local stimulation of sensory afferent nerve fiber growth in the skin is investigated using an *in-vitro* co-culture system of porcine DRGs and human primary skin cells.

First, the co-culture system is characterized according to its sensitivity to recombinant human NGFβ and the subtypes of sensory fibers outgrown. The functionality of cultured sensory neurons is verified via unspecific and specific stimulation and the detection of released neuropeptides.

Second, the effects of primary human skin cells on the outgrowth of peripheral sensory fibers is examined. The expression and production of endogenous NGF of keratinocytes and fibroblasts is detected and correlated with induced fiber growth. Furthermore, the application of an anti-NGF antibody specifically blocks the trophic effects mediated by endogenous NGF and allows for the identification of NGF independent fiber growth mediated by skin cells.

5.1 The co-culture system

In-vivo the cell bodies of sensory afferent neurons are located in the ganglia of the dorsal root and the cranial nerves. These pseudounipolar cells are clustered together without dendritic interconnections and surrounded only by glia cells, referred to as satellite cells [103]. In contrast, sensory nerve fibers in the skin interact and are associated with multiple different cell types including keratinocytes, fibroblasts, endothelial cells, Merkel cells, Langerhans cells and mast cells [34]. They form an extensive three dimensional network in the dermis and epidermis [12] and are exposed to and express receptors for a multitude of neurotrophic factors, neuropeptides and cytokines [34]. Free nerve endings (FNEs) accumulate vesicles and cytoplasmic organelles and release various neuropeptides themselves [105]. Thus, where the neuronal somata are rather isolated and dependent on satellite cells and retrograd transport of survival factors, their peripheral terminal endings widely interact with the cells of the target tissue. Current mixed *in-vitro* models of peripheral sensory neurons and skin cells [94] are inadequate as they do not account for the anatomical spatial separation and the different molecular microenvironments of somata and nerve fiber endings.

The present co-culture system was developed to more accurately mimic the *in-vivo* situation. The neuronal somata and their axonal processes are cultivated in separate

compartments, sealed by silicon and a sugar polymer mixture. „Peripheral" axonal processes are able to grow from the middle into the side compartments and cultivation conditions are optimized for both, neuronal and human skin cells.

For obvious reason, human DRGs are not available for the co-culture system. However, murine and rat sensory neurons have been shown to significantly differ in several sensory neuronal channels, for instance in the expression of Mas-related G-protein coupled receptors (Mrgprs) [14]. In addition, the expression of molecular markers as IB4, CGRP and SP and therefore the diversification of nociceptive neurons varies considerably with species [28]. Furthermore, human skin differs from rat skin in several aspects of neurogenic inflammation [24]. In recent years, the pig *sus scrofa domestica* gained significance as an alternative model organism to rodents in neuroscience, as there is substantial similarity between human and pig neuronal anatomy, physiology [106] and pharmacology [107]. In order to establish an *in-vitro* model that closely reproduces the *in-vivo* situation in human skin, porcine DRGs and human primary skin cells were combined.

5.1.1 Effect of recombinant growth factors on sensory nerve growth

The co-culture system is sufficiently sensitive to induce peripheral fiber outgrowth in response to neurotrophic factors. Here, recombinant human NGFβ was applied to the side compartments in increasing concentrations and mediated peripheral neurite outgrowth in a dose dependent manner. A minimum of 40 pg/mL were sufficient for 26,464 ±2,217 mm cumulative peripheral fiber growth (CPNL), whereas the high standard positive control of 10 ng/mL induced a CPNL of 17,997 ±1,046 cm at day 10. In general, axonal processes appeared in the side compartment at day 4 to 5 and showed largest increase in total length between day 6 and 10. The length of a single axonal process varied between several µm and up to one cm. Results strongly indicate, that the present co-culture system is well fit to study attractive as well as repellent trophic effects on sensory neuronal growth of any given soluble factor.

5.1.2 Quantitative analysis of nociceptive molecular markers in the peripheral fibers

Dorsal root ganglion cells have been extensively characterized according to the expression of nociceptive molecular markers as NF200, IB4, SP, CGRP, TrkA and

TRPV1 [28]. Beside immunofluorescent studies, a combination of fluorescent labeling and electrophysiology has been applied to relate molecular marker expression to function [32]. Additionally, sensory neuronal afferents in the skin are detected via immunohistochemical studies [108]. However, the quantitative detection of molecular marker expression on neuronal fibers in the skin is challenging. Several markers are as well expressed on skin cells and cause significant „background" staining. For example, keratinocytes express and stain positive for TrkA and TRPV1 [34]. Furthermore, vertical sections of the skin cut through the three dimensional sensory network, and require sequential cutting and computational reconstruction to suffice a quantitative approach [14].

In the present co-culture system neuronal somata and their peripheral fibers are cultivated in spatially separated compartments. In addition to the detection of nociceptive markers expressed by DRGs, it is possible to quantify the expression of individual markers in the sensory fibers. Quantitative changes in the expression pattern as response to different peripheral growth conditions can be detected and analyzed.

Here, the expression of the nociceptive markers IB4, CGRP, TrkA and TRPV1 was quantified in periperal afferent fibers grown in response to recombinant huNGFβ. IB4 and CGRP expression was prevailing with 63,8 % and 54,7 %, respectively. These values strongly indicate a significant overlap between the two markers in peripheral sensory afferents, as it has been shown for DRGs [28]. However, double staining of both markers for the verification and quantification of the overlap is pending. The NGF high affinity receptor TrkA was detected along 17,8 % and TRPV1 at 4,6 % of CPNL. The small relative number of TRPV1 expression may at least in part be explained by the nature of its expression pattern. The TRPV1 signal was confined to the fiber endings, whereas IB4, CGRP and TrkA were observed alongside the axonal shafts. Thus, besides the relative values of CPNL positive for individual molecular markers, a qualitative conclusion of the expression pattern can be drawn.

5.1.3 Specific and unspecific stimulation of efferent functions of sensory neurons

Besides their various receptive properties, sensory neuronal afferents are able to release neurotransmitters, neuropeptides and neurohormones [34]. In the skin, this local efferent function of sensory afferent neurons is involved in a complex auto and

para-neuroendocrine system between nerve fibers, skin cells, immune cells and the microvascular system [24] [33] [34].

Two distinct mechanisms for the efferent release of neuropeptides have been described. The classical model of the *axon reflex* was first proposed by Lewis 1927 [109] and originally associated with vasodilatation and plasma extravasation during the weal and flare response to focal skin irritation. To date, the concept has been expanded to neurogenic inflammation in general, including also non-vascular effects mediated by neuropeptide release, sensitization of sensory afferents and immune cell activation [110] [36]. Peripheral sensory afferent depolarization results in a pulse that travels centrally, but induces antidromically proceeding signals at branching points of the same neuron. Antidromic signals travel back to the periphery and result in the release of neuromediators from the fiber endings. However, this picture is incomplete as the induction of peripheral flare response by histamine injection [111] and cutaneous inflammation following capsaicin injection [104] is abolished by removal of DRGs and distal dorsal root rhizotomy, respectively. Intact DRGs and the involvement of neuronal somata seem crucial to efferent functions of sensory afferents mediated by axon reflex.

As direct stimulation of the dorsal root was shown to induce antidromic vasodilatation [109] [112], a similar approach was chosen to test the functionality of sensory neurons grown in the present co-culture system. The cell somata in the middle compartment were subjected to stimulus application, whereas the efferent release of neuropeptides of the peripheral fibers in the side compartment was detected.

The neuropeptide CGRP is considered the most abundant neuropeptide in Aδ and C fibers in the human skin [50]. It constitutes the predominant neuropeptide in DRGs expressed by approximately 40 % of the somata (*rattus norvegicus*) [34] and is expressed by 63,8 % of peripheral CPNL in the present co-culture system (5.1.2). Therefore, the efferent release of CGRP into the supernatant was chosen as the readout parameter.

Neuropeptides are released from C and Aδ fibers in response to a wide range of internal and external stimuli. Intradermal injection of capsaicin mediates neurogenic inflammation via the axon reflex mechanism and involves the peripheral release of SP and CGRP [104]. In the same setup, neurogenic inflammation is completely abolished by the application of the TRPV1 antagonist capsazepine in a dose dependent manner.

In the present co-culture system the capsaicin receptor TRPV1 is expressed by neuronal somata. Therefore, capsaicin and capsazepine were chosen for the specific, receptor mediated stimulation and block of CGRP release, respectively. Unspecific stimulation with high potassium (50 mM) was used as positive control [99].

Both, unspecific high potassium and specific capsaicin mediated stimulation of neuronal somata resulted in efferent CGRP release in the side compartment. High potassium application yielded an approximately 20-fold increase in CGRP levels compared to basal release. Repetitive stimulation was accomplished, however basal CGRP levels between two cycles did not completely return to the initial basal level. Specific stimulation with capsaicin resulted in a 2,3-fold increase in the peripheral CGRP levels, whereas the co-application of capsaicin and capsazepine did not stimulate CGRP release above the basal level. Thus, capsazepine specifically blocked capsaicin mediated CGRP release, whereas the co-application of high potassium and capsazepine yielded a 2,2-fold increase in CGRP levels.

In addition to the axon reflex concept, the direct release of neuromediators from the stimulated sensory afferent terminals of capsaicin sensitive neurons has been shown [113]. This local *coupling* of the afferent and efferent function of sensory neurons plays a key role in the intercellular crosstalk and skin homeostasis. Although these experiments have not been performed in the present thesis, direct stimulation of the peripheral fibers is also feasible.

Since DRGs are spatially separated from the peripheral fibers, it seems further possible to investigate changes in the peripheral efferent functions during application of central acting substances. An equivalent mechanism *in-vivo* is the presynaptic inhibition of the central projections of primary afferent neurons in the spinal cord [110].

CGRP positive afferent fibers in the skin are often associated with keratinocytes, melanocytes [54], Merkel cells, Langerhans cells [55] or mast cells [56]. These cell types also play an important role in inflammatory conditions [34]. Using the co-culture system, the investigation of efferent functions of sensory afferents in co-culture with virtually any other cutaneous cell type is possible. Notably, the efferent release of neuromediators from peripheral fibers may be directly quantified in the supernatant.

5.2 Neurotrophic effects of human skin cells on sensory neurons

In several cutaneous diseases significant changes in the epidermal neuronal fiber density and morphology has been detected. In atopic dermatitis (AD) and Psoriasis peptidergic SP$^+$ CGRP$^+$ fiber density is increased [89] [88], wherease diabetic neuropathy shows a reduction in unmyelinated epidermal C fibers [114]. Consistently, the level of NGF is elevated in AD [108] and psoriasis [115], and depleted in the skin of early diabetic neuropathy [70] [116]. Further, NGF regulates the production of neuropeptides in sensory afferents. Neuropeptides have an influence on the production and release of cytokines, as TNFα, IL-1 and INFγ that in turn stimulate the cutaneous expression of NGF, NT-3 and NT-4 [117]. Thus, a strong neurogenic component is suggested in the development and sustainment of cutaneous diseases.

In this thesis, the local influence of primary human dermal and epidermal skin cells on sensory afferent nerve growth is investigated using the co-culture system. Both, keratinocytes and fibroblasts were sufficient to induce sensory fiber outgrowth. Surprisingly, keratinocyte mediated outgrowth exceeded the CPNL of the high standard 10 ng/mL recombinant huNGFβ, though not significantly. Fibroblasts induced substantial peripheral fiber growth, however only 25 % of the CPNL mediated by keratinocytes.

The concentration of endogenously produced NGFβ of primary skin cells in the co-culture chamber was detected in parallel. The supernatants of keratinocytes and fibroblasts contained similar concentrations of average 23,8 pg/mL and 19,4 pg/mL NGFβ, respectively. However, the NGFβ concentrations did not correlate with induced total fiber outgrowth. Keratinocytes induced an average CPNL of 247,9 mm, whereas fibroblasts only mediated 44,9 mm. Furthermore, the 500-times higher concentration of 10 ng/mL recombinant huNGFβ induced an average CPNL of 180 mm, which is 4-times the CPNL obtained by fibroblasts, but only 0,7-times that of keratinocytes.

Although differences in the trophic capacity between endogenously and recombinantly produced huNGFβ are possible, the vast difference in CPNL of keratinocytes and fibroblasts occurred in the presence of equal concentrations of endogenous NGFβ. The involvement of at least one other keratinocyte derived component seemed likely to account for this difference.

To identify potential NGF independent fiber growth, a specific anti-NGFβ antibody was co-applied with primary skin cells to inhibit the biological effects of endogenous NGFβ. The CPNL of fibroblasts decreased to the negative control level in the presence of the antibody, whereas keratinocytes mediated 42,9 % NGF independent CPNL. Hence, keratinocytes and fibroblasts showed significant difference in NGFβ dependency to promote neurite growth. Whereas fibroblast mediated outgrowth is considered to be dependent on NGFβ, only 57,1 % of keratinocyte mediated CPNL is. The results were reproducible with conditioned media. Thus, NGF independent keratinocyte mediated growth is likely caused by at least one additional soluble factor.

5.2.1 Difference in morphology of peripheral fibers mediated by keratinocytes and fibroblasts

Differences in the trophic effects of keratinocytes and fibroblasts on fiber outgrowth were also detectable via immunofluorescent analysis. Neurites stimulated by keratinocytes exhibited extensive branching and fibers wrapped around individual cells. No difference in morphology was detected between keratinocyte induced neurites and NGF independent keratinocyte induced neurites (data not shown). On the other hand, fibroblasts mediated peripheral fibers of an unbranched, straight phenotype with minor wrapping. Thus, besides the distinct dependency on NGF for the induction of fiber growth, both cell types exert crucial influence on the local morphology of sensory afferents.

5.2.2 Kinetics of NGF independent growth mediated by keratinocytes

In addition, the kinetics of fiber outgrowth induced by keratinocytes with and without anti-NGFβ antibody was significantly different. No difference in CPNL was detected at day 4 and 6. However, at day 10 NGF independent CPNL scores only 42,9 % compared to fiber growth in the presence of endogenous NGFβ. Neurites entered the keratinocyte layer of the co-culture system approximately at day 6.

It is concluded that NGFβ is not necessary for neurites to enter the side compartments, extend and reach the keratinocyte layer. In general, increase in CPNL is most prominent between day 6 and 10, as shown in growth curves with external huNGFβ. It is hypothesized that NGFβ is mainly necessary for the increase and growth in length, in consistence with the immunofluorescent analysis of neurite morphology (5.2.1).

5.3 Potential additional keratinocyte derived factors in sensory fiber outgrowth – GDNF

Glial cell-line derived neurotrophic factor is a distant member of the TGFβ superfamily based on structural and conformational similarities. The active homodimer binds the GDNF family receptor α (GFRα1), induces recruitment and autophosphorylation of the receptor tyrosine kinase Ret and intracellular signaling via Src kinase [118]. Approximately half of the TrkA[+], NGF dependent DRGs switch their expression pattern and dependency towards GDNF in early postnatal life [31]. Subsequently, GDNF mediates the survival of IB4 positive, non-peptidergic, small diameter sensory afferents of both the somatosensory and the autonomic nervous system [119].

Immunofluorescent analysis and RT-PCR of human skin showed strong expression of GDNF, GFRα1/2 and Ret in all epidermal layers, whereas GDNF gradually decreases with ascending keratinocyte layers [65]. In addition, preliminary data obtained in this thesis via real time PCR of primary human skin cells, revealed equal expression levels of GDNF and NGF in keratinocytes. In human fibroblasts GDNF expression was significantly lower than NGF expression, though still higher than the GDNF level measured in keratinocytes (preliminary data, not shown).

Additionally, GDNF is implicated in cutaneous diseases as AD, inflammation and hyperalgesia. GDNF production was found enhanced in the epidermis of two distinct mouse models of atopic dermatitis [120]. Injection and overexpression of GDNF in the skin of rat [121] and mouse [122] significantly reduced the thresholds of mechanical stimulation and led to sensitization of nociceptors and mechanical hyperalgesia. Furthermore, inflammatory conditions induced by radiant heat led to gradually enhanced secretion of GDNF in DRGs and induced a specific increase in TRPV1 expression on IB4 positive neurons [82].

Taken together, GDNF would present a quite reasonable candidate for the detected induction of NGF independent peripheral fiber growth mediated by keratinocytes. Further experiments are needed to determine the potential of GDNF to stimulate fiber outgrowth and the induced sensory fiber types. Subsequent combinations of anti-NGF and anti-GDNF antibodies co-applied with keratinocytes allow the quantification of GDNF dependent peripheral sensory afferents.

6   Abstract

In this work, the local influence of dermal and epidermal skin cells on sensory afferent nerve growth was investigated using a novel *in-vitro* co-culture system of porcine dorsal root ganglion cells (DRGs) and human primary skin cells.

The co-culture system allows for the cultivation of cell somata and peripheral neuronal processes in spatially separated compartments that are liquid-impermeable. In accordance with the *in-vivo* situation, only the axonal processes of sensory neurons were co-cultivated with dermal and epidermal skin cells in the „peripheral" compartment. This approach allows to study the neuronal cutaneous network *in-vitro*.

In a first attempt, the co-culture system was established and characterized. The sensitivity of the system in response to the neurotrophic factor human NGFβ was examined. Recombinant huNGFβ induced a dose-dependent outgrowth of peripheral sensory fibers in a range between several pg/mL to 10 ng/mL. The major increase in cumulative peripheral neurite length (CPNL) was detected between day 6 and 10 of cells in culture.

Subsequently, subtypes of peripheral sensory fibers grown in response to huNGFβ were characterized and quantified via immunofluorescent staining for the nociceptive, peptidergic markers calcitonin-gene-related-peptide (CGRP) and receptor tyrosine kinase TrkA, the non-peptidergic marker Isolectin B4 (IB4) and the vanilloid receptor TRPV1. IB4 and CGRP expressions were prevailing with 63,8 % and 54,7 %, followed by TrkA with 17,8 % and TRPV1 with 4,6 % of CPNL, thus confirming the nociceptive sensory phenotype of the grown fibers.

The functionality of the cultured sensory neurons was verified via unspecific stimulation with high potassium (50mM) and specific stimulation with the TRPV1 agonist capsaicin (CPS) and inhibition with the antagonist capsazepine (CPZ), respectively. Unspecific and specific stimulation of the somata in the middle compartment resulted in an efferent release of the neuropeptide CGRP in the peripheral side compartment. The CPS mediated stimulation of TRPV1 was successfully inhibited by the receptor specific antagonist CPZ, further emphasizing the functionality of the cultured neurons.

Finally, the neurotrophic effects of keratinocytes and fibroblasts on peripheral sensory fiber outgrowth was investigated. Both cell types were sufficient to induce substantial

sensory fiber outgrowth. Surprisingly, keratinocyte mediated CPNL exceeded the outgrowth mediated by recombinant huNGFβ.

Additionally, co-application of an anti-NGFβ antibody decreased fibroblast mediated growth to negative control level, whereas keratinocytes mediated growth was only reduced to 42,9 %. These results indicate that fibroblasts induce fiber growth mainly via NGF, whereas keratinocytes produce at least one additional soluble factor that accounts for the NGF independent fiber growth.

Comparison of keratinocyte mediated outgrowth with and without anti-NGFβ antibody revealed no difference in CPNL values at day 4 and 6. As neuronal fibers usually reached the keratinocyte layer at day 6, NGF seems not necessary for neurites to enter the side compartment, extend and reach the keratinocytes. NGF may rather play a role for the increase in length between day 6 and 10, consistent with the reduction of 57,1 % of CPNL without NGF.

Further consistent with this hypothesis was the analysis of fiber morphology. Neurites stimulated by keratinocytes exhibited extensive branching and frequently wrapped around individual cells. On the contrary, fibroblasts mediated fibers of more unbranched and straight phenotype.

7   Zusammenfassung

Im Rahmen dieser Arbeit wurde der Einfluss von dermalen und epidermalen Hautzellen auf das Wachstum von peripheren sensorischen Nerven in einem neuen *in-vitro* Kokultur-Modell untersucht.

In diesem Modell werden neuronale Zellkörper und ihre peripheren Fortsätze örtlich getrennt in separaten, flüssigkeitsdichten Kammern kultiviert. Entsprechend den Gegebenheiten *in-vivo*, wurden dermale und epidermale Hautzellen ausschließlich mit den neuronalen Fortsätzen in der „peripheren" Seitenkammer kultiviert. Dieses spezielle Setup ermöglicht die Untersuchung des peripheren neuronalen Netzwerks in der Haut *in-vitro*.

Im ersten Schritt der Arbeit wurde das Kokultur-Modell etabliert und charakterisiert. Die Sensitivität des Systems auf neurotrophe Faktoren wurde mittels humanem NGFβ analysiert. Rekombinantes huNGFβ induzierte dosis-abhängiges peripheres Neuritenwachstum in einem Bereich von wenigen pg/mL bis hin zu 10 ng/mL. Die größte Zunahme an der gesamten peripheren Neuriten Länge (*cumulative peripheral neurite length*, CPNL) wurde zwischen dem sechsten und zehnten Tag der Kultivierung beobachtet.

Die von huNGFβ induzierten peripheren Fortsätze wurden im Anschluss mittels Immunfluoreszenzfärbung charakterisiert und quantifiziert. Detektiert wurden die Marker für sensorische, nozizeptive, peptiderge Neurone *Calcitonin-gene-related-peptide* (CGRP) und *Receptor tyrosine kinase* TrkA, der sensorische, nozizeptive, nicht-peptiderge Marker *Isolectin B4* (IB4) und der Vanilloid Rezeptor TRPV1. Die Espression von IB4 und CGRP war mit 63,8 % und 54,7 % am stärksten detektiertbar, gefolgt von TrkA mit 17,8 % und TRPV1 mit 4,6 %. Der positive Nachweis dieser Marker bestätigt die Präsenz von sensorischen, nozizeptiven Fasern im vorliegenden Modell. Dabei kann zum ersten Mal eine quantitative Aussage über das Expressionsmuster dieser Marker in den peripheren Fasern, abhängig von den Wachstumsbedingungen gemacht werden.

Die Funktionalität der kultivierten Neuronen wurde mittels unspezifischer Stimulation mit 50 mM Kalium und spezifischer Stimulation mit dem TRPV1 Agonisten Capsaicin (CPS), sowie Inhibition mit dem Antagonisten Capsazepin (CPZ) bestätigt. Sowohl unspezifische als auch spezifische Stimulation der neuronalen Somata in der Mittelkammer bewirkten die efferente Ausschüttung des Neuropeptids CGRP in der

peripheren Seitenkammer. Die Stimulation von TRPV1 mittels CPS wurde erfolgreich durch den Rezeptor-spezifischen Antagonisten CPZ inhibiert und bestätigt erneut die Funktionalität der kultivierten Neurone.

Schließlich wurde die neurotrophe Wirkung von Fibroblasten und Keratinozyten auf das Wachstum der peripheren neuronalen Fortsätze untersucht. Beide Zelltypen induzierten erhebliches Neuritenwachstum, wobei Keratinozyten sogar höhere CPNL Werte erzielte als recombinantes huNGFβ. Bei gleichzeitiger Anwendung eines anti-NGFβ Antikörpers wurde das von Fibroblasten induzierte Wachstum auf Kontrollniveau reduziert, wohingegen Keratinozyten vermitteltes Wachstum nur auf 42,9 % verringert wurde. Diese Ergebnisse deuten darauf hin, dass Fibroblasten induziertes Neuritenwachstum größtenteils durch NGF vermittelt wird. Keratinozyten scheinen hingegen zumindest einen zustätzlichen, sekretierten Faktor zu produzieren, der für das verbleibende, NGF unabhängige Wachstum verantwortlich ist.

Im Vergleich zwischen Keratinozyten vermitteltem Neuritenwachstum mit und ohne anti-NGFβ Antikörper, zeigte sich keinerlei Unterschied in den CPNL Werten am Tag 4 und 6. Da Neurite üblicherweise die Keratinozytenschicht am Tag 6 erreichen, scheint NGF nicht notwendig für das Auswachsen und Erreichen der Keratinozyten zu sein. NGF spielt möglicherweise eine größere Rolle im Längenwachstum zwischen Tag 6 und 10, wo sich ein Unterschied von minus 57,1 % ohne NGF manifestiert.

Mit dieser Annahme gehen auch Beobachtungen der Morphology der Neurite konform. Keratinozyten vermittelten Fortsätze mit einem hohen Grad an Verzweigungen, die häufig einzelne Zellen umwickelten. Hingegen wiesen Fibroblasten induzierte Fasern einen geradlinigen, gering verzweigten Phänotyp auf.

8 References

[1] John Harry Martin HJR, Michael E. Leonard. Neuroanatomy: Text and Atlas March 2003.

[2] Reznik M. [Structure and functions of the cutaneous nervous system]. *Pathol Biol (Paris)*. 1996;**44**:831-7.

[3] Tandrup T. Are the neurons in the dorsal root ganglion pseudounipolar? A comparison of the number of neurons and number of myelinated and unmyelinated fibres in the dorsal root. *J Comp Neurol*. 1995;**357**:341-7.

[4] Weber KT, Sun Y, Katwa LC. Local regulation of extracellular matrix structure. *Herz*. 1995;**20**:81-8.

[5] Kretsos K, Kasting GB. Dermal capillary clearance: physiology and modeling. *Skin Pharmacol Physiol*. 2005;**18**:55-74.

[6] Salmon JK, Armstrong CA, Ansel JC. The skin as an immune organ. *West J Med*. 1994;**160**:146-52.

[7] Vetrugno R, Liguori R, Cortelli P, Montagna P. Sympathetic skin response: basic mechanisms and clinical applications. *Clin Auton Res*. 2003;**13**:256-70.

[8] Tschachler E, Reinisch CM, Mayer C, Paiha K, Lassmann H, Weninger W. Sheet preparations expose the dermal nerve plexus of human skin and render the dermal nerve end organ accessible to extensive analysis. *J Invest Dermatol*. 2004;**122**:177-82.

[9] Nurse CA, Mearow KM, Holmes M, Visheau B, Diamond J. Merkel cell distribution in the epidermis as determined by quinacrine fluorescence. *Cell Tissue Res*. 1983;**228**:511-24.

[10] Allombert-Blaise C, Tamiji S, Mortier L, et al. Terminal differentiation of human epidermal keratinocytes involves mitochondria- and caspase-dependent cell death pathway. *Cell Death Differ*. 2003;**10**:850-2.

[11] Candi E, Schmidt R, Melino G. The cornified envelope: a model of cell death in the skin. *Nat Rev Mol Cell Biol*. 2005;**6**:328-40.

[12] Reilly DM, Ferdinando D, Johnston C, Shaw C, Buchanan KD, Green MR. The epidermal nerve fibre network: characterization of nerve fibres in human skin by confocal microscopy and assessment of racial variations. *Br J Dermatol*. 1997;**137**:163-70.

[13] Lauria G. Innervation of the human epidermis. A historical review. *Ital J Neurol Sci*. 1999;**20**:63-70.

[14] Zylka MJ, Rice FL, Anderson DJ. Topographically distinct epidermal nociceptive circuits revealed by axonal tracers targeted to Mrgprd. *Neuron*. 2005;**45**:17-25.

[15] Lawson SN. Phenotype and function of somatic primary afferent nociceptive neurones with C-, Adelta- or Aalpha/beta-fibres. *Exp Physiol*. 2002;**87**:239-44.

[16] Singh G. The muscle spindle- an anatomical and physiological appraisal. *Singapore Med J*. 1978;**19**:48-52.

[17] Lumpkin EA, Caterina MJ. Mechanisms of sensory transduction in the skin. *Nature*. 2007;**445**:858-65.

[18] Voets T, Talavera K, Owsianik G, Nilius B. Sensing with TRP channels. *Nat Chem Biol*. 2005;**1**:85-92.

[19] Gomis A, Soriano S, Belmonte C, Viana F. Hypoosmotic- and pressure-induced membrane stretch activate TRPC5 channels. *J Physiol*. 2008;**586**:5633-49.

[20]   Levine JD, Alessandri-Haber N. TRP channels: targets for the relief of pain. *Biochim Biophys Acta*. 2007;**1772**:989-1003.

[21]   St Pierre M, Reeh PW, Zimmermann K. Differential effects of TRPV channel block on polymodal activation of rat cutaneous nociceptors in vitro. *Exp Brain Res*. 2009.

[22]   Biro T, Toth BI, Marincsak R, Dobrosi N, Geczy T, Paus R. TRP channels as novel players in the pathogenesis and therapy of itch. *Biochim Biophys Acta*. 2007;**1772**:1004-21.

[23]   Starowicz K, Nigam S, Di Marzo V. Biochemistry and pharmacology of endovanilloids. *Pharmacol Ther*. 2007;**114**:13-33.

[24]   Stephen McMahon MK. Textbook of Pain. 5 ed: A Churchill Livingstone Title 2005.

[25]   Pezet S, McMahon SB. Neurotrophins: mediators and modulators of pain. *Annu Rev Neurosci*. 2006;**29**:507-38.

[26]   Fullmer JM, Riedl MS, Higgins L, Elde R. Identification of some lectin IB4 binding proteins in rat dorsal root ganglia. *Neuroreport*. 2004;**15**:1705-9.

[27]   Bogen O, Dreger M, Gillen C, Schroder W, Hucho F. Identification of versican as an isolectin B4-binding glycoprotein from mammalian spinal cord tissue. *FEBS J*. 2005;**272**:1090-102.

[28]   Price TJ, Flores CM. Critical evaluation of the colocalization between calcitonin gene-related peptide, substance P, transient receptor potential vanilloid subfamily type 1 immunoreactivities, and isolectin B4 binding in primary afferent neurons of the rat and mouse. *J Pain*. 2007;**8**:263-72.

[29]   Zylka MJ, Dong X, Southwell AL, Anderson DJ. Atypical expansion in mice of the sensory neuron-specific Mrg G protein-coupled receptor family. *Proc Natl Acad Sci U S A*. 2003;**100**:10043-8.

[30]   Molliver DC, Snider WD. Nerve growth factor receptor TrkA is down-regulated during postnatal development by a subset of dorsal root ganglion neurons. *J Comp Neurol*. 1997;**381**:428-38.

[31]   Molliver DC, Wright DE, Leitner ML, et al. IB4-binding DRG neurons switch from NGF to GDNF dependence in early postnatal life. *Neuron*. 1997;**19**:849-61.

[32]   Stucky CL, Lewin GR. Isolectin B(4)-positive and -negative nociceptors are functionally distinct. *J Neurosci*. 1999;**19**:6497-505.

[33]   Scholzen T, Armstrong CA, Bunnett NW, Luger TA, Olerud JE, Ansel JC. Neuropeptides in the skin: interactions between the neuroendocrine and the skin immune systems. *Exp Dermatol*. 1998;**7**:81-96.

[34]   Roosterman D, Goerge T, Schneider SW, Bunnett NW, Steinhoff M. Neuronal control of skin function: the skin as a neuroimmunoendocrine organ. *Physiol Rev*. 2006;**86**:1309-79.

[35]   Peters EM, Ericson ME, Hosoi J, et al. Neuropeptide control mechanisms in cutaneous biology: physiological and clinical significance. *J Invest Dermatol*. 2006;**126**:1937-47.

[36]   Steinhoff M, Stander S, Seeliger S, Ansel JC, Schmelz M, Luger T. Modern aspects of cutaneous neurogenic inflammation. *Arch Dermatol*. 2003;**139**:1479-88.

[37]   Hendrix S, Peters EM. Neuronal plasticity and neuroregeneration in the skin -- the role of inflammation. *J Neuroimmunol*. 2007;**184**:113-26.

[38] Steinhoff M, Bienenstock J, Schmelz M, Maurer M, Wei E, Biro T. Neurophysiological, neuroimmunological, and neuroendocrine basis of pruritus. *J Invest Dermatol*. 2006;**126**:1705-18.

[39] Strand VFL. Neuropeptides: regulators of physiological processes: MIT Press 1999.

[40] Dalsgaard CJ, Haegerstrand A, Theodorsson-Norheim E, Brodin E, Hokfelt T. Neurokinin A-like immunoreactivity in rat primary sensory neurons; coexistence with substance P. *Histochemistry*. 1985;**83**:37-9.

[41] Moller K, Zhang YZ, Hakanson R, et al. Pituitary adenylate cyclase activating peptide is a sensory neuropeptide: immunocytochemical and immunochemical evidence. *Neuroscience*. 1993;**57**:725-32.

[42] Wimalawansa SJ. Amylin, calcitonin gene-related peptide, calcitonin, and adrenomedullin: a peptide superfamily. *Crit Rev Neurobiol*. 1997;**11**:167-239.

[43] Johansson O, Ljungberg A, Han SW, Vaalasti A. Evidence for gamma-melanocyte stimulating hormone containing nerves and neutrophilic granulocytes in the human skin by indirect immunofluorescence. *J Invest Dermatol*. 1991;**96**:852-6.

[44] Millington GW. Proopiomelanocortin (POMC): the cutaneous roles of its melanocortin products and receptors. *Clin Exp Dermatol*. 2006;**31**:407-12.

[45] Ralevic V. Cannabinoid modulation of peripheral autonomic and sensory neurotransmission. *Eur J Pharmacol*. 2003;**472**:1-21.

[46] Hoppener JW, Steenbergh PH, Slebos RJ, et al. Expression of the second calcitonin/calcitonin gene-related peptide gene in Ewing sarcoma cell lines. *J Clin Endocrinol Metab*. 1987;**64**:809-17.

[47] Sternini C. Tachykinin and calcitonin gene-related peptide immunoreactivities and mRNAs in the mammalian enteric nervous system and sensory ganglia. *Adv Exp Med Biol*. 1991;**298**:39-51.

[48] Hay DL. What makes a CGRP2 receptor? *Clin Exp Pharmacol Physiol*. 2007;**34**:963-71.

[49] Bennett DL, Dmietrieva N, Priestley JV, Clary D, McMahon SB. trkA, CGRP and IB4 expression in retrogradely labelled cutaneous and visceral primary sensory neurones in the rat. *Neurosci Lett*. 1996;**206**:33-6.

[50] Gibbins IL, Wattchow D, Coventry B. Two immunohistochemically identified populations of calcitonin gene-related peptide (CGRP)-immunoreactive axons in human skin. *Brain Res*. 1987;**414**:143-8.

[51] Wallengren J, Ekman R, Sundler F. Occurrence and distribution of neuropeptides in the human skin. An immunocytochemical and immunochemical study on normal skin and blister fluid from inflamed skin. *Acta Derm Venereol*. 1987;**67**:185-92.

[52] Brain SD, Grant AD. Vascular actions of calcitonin gene-related peptide and adrenomedullin. *Physiol Rev*. 2004;**84**:903-34.

[53] Haegerstrand A, Dalsgaard CJ, Jonzon B, Larsson O, Nilsson J. Calcitonin gene-related peptide stimulates proliferation of human endothelial cells. *Proc Natl Acad Sci U S A*. 1990;**87**:3299-303.

[54] Hara M, Toyoda M, Yaar M, et al. Innervation of melanocytes in human skin. *J Exp Med*. 1996;**184**:1385-95.

[55] Hosoi J, Murphy GF, Egan CL, et al. Regulation of Langerhans cell function by nerves containing calcitonin gene-related peptide. *Nature*. 1993;**363**:159-63.

[56]   Botchkarev VA, Eichmuller S, Peters EM, et al. A simple immunofluorescence technique for simultaneous visualization of mast cells and nerve fibers reveals selectivity and hair cycle--dependent changes in mast cell--nerve fiber contacts in murine skin. *Arch Dermatol Res*. 1997;**289**:292-302.

[57]   Clementi G, Caruso A, Cutuli VM, et al. Anti-inflammatory activity of amylin and CGRP in different experimental models of inflammation. *Life Sci*. 1995;**57**:PL193-7.

[58]   Ansel JC, Armstrong CA, Song I, et al. Interactions of the skin and nervous system. *J Investig Dermatol Symp Proc*. 1997;**2**:23-6.

[59]   Niizeki H, Alard P, Streilein JW. Calcitonin gene-related peptide is necessary for ultraviolet B-impaired induction of contact hypersensitivity. *J Immunol*. 1997;**159**:5183-6.

[60]   Cunha FQ, Ferreira SH. Peripheral hyperalgesic cytokines. *Adv Exp Med Biol*. 2003;**521**:22-39.

[61]   Levi-Montalcini R, Angeletti PU. Nerve growth factor. *Physiol Rev*. 1968;**48**:534-69.

[62]   Watson FL, Heerssen HM, Moheban DB, et al. Rapid nuclear responses to target-derived neurotrophins require retrograde transport of ligand-receptor complex. *J Neurosci*. 1999;**19**:7889-900.

[63]   Neet KE, Campenot RB. Receptor binding, internalization, and retrograde transport of neurotrophic factors. *Cell Mol Life Sci*. 2001;**58**:1021-35.

[64]   Di Marco E, Marchisio PC, Bondanza S, Franzi AT, Cancedda R, De Luca M. Growth-regulated synthesis and secretion of biologically active nerve growth factor by human keratinocytes. *J Biol Chem*. 1991;**266**:21718-22.

[65]   Adly MA, Assaf HA, Hussein MR, Paus R. Analysis of the expression pattern of glial cell line-derived neurotrophic factor, neurturin, their cognate receptors GFRalpha-1 and GFRalpha-2, and a common signal transduction element c-Ret in the human scalp skin. *J Cutan Pathol*. 2006;**33**:799-808.

[66]   Hattori A, Iwasaki S, Murase K, et al. Tumor necrosis factor is markedly synergistic with interleukin 1 and interferon-gamma in stimulating the production of nerve growth factor in fibroblasts. *FEBS Lett*. 1994;**340**:177-80.

[67]   Gibran NS, Tamura R, Tsou R, Isik FF. Human dermal microvascular endothelial cells produce nerve growth factor: implications for wound repair. *Shock*. 2003;**19**:127-30.

[68]   Nosrat CA, Tomac A, Hoffer BJ, Olson L. Cellular and developmental patterns of expression of Ret and glial cell line-derived neurotrophic factor receptor alpha mRNAs. *Exp Brain Res*. 1997;**115**:410-22.

[69]   Vos P, Stark F, Pittman RN. Merkel cells in vitro: production of nerve growth factor and selective interactions with sensory neurons. *Dev Biol*. 1991;**144**:281-300.

[70]   Anand P. Neurotrophic factors and their receptors in human sensory neuropathies. *Prog Brain Res*. 2004;**146**:477-92.

[71]   Fahnestock M. Structure and biosynthesis of nerve growth factor. *Curr Top Microbiol Immunol*. 1991;**165**:1-26.

[72]   Shooter EM. Early days of the nerve growth factor proteins. *Annu Rev Neurosci*. 2001;**24**:601-29.

[73]   Bax B, Blundell TL, Murray-Rust J, McDonald NQ. Structure of mouse 7S NGF: a complex of nerve growth factor with four binding proteins. *Structure*. 1997;**5**:1275-85.

[74] Al-Shawi R, Hafner A, Chun S, et al. ProNGF, sortilin, and age-related neurodegeneration. *Ann N Y Acad Sci*. 2007;**1119**:208-15.

[75] Bruno MA, Cuello AC. Activity-dependent release of precursor nerve growth factor, conversion to mature nerve growth factor, and its degradation by a protease cascade. *Proc Natl Acad Sci U S A*. 2006;**103**:6735-40.

[76] Barrett GL. The p75 neurotrophin receptor and neuronal apoptosis. *Prog Neurobiol*. 2000;**61**:205-29.

[77] Jullien J, Guili V, Derrington EA, Darlix JL, Reichardt LF, Rudkin BB. Trafficking of TrkA-green fluorescent protein chimerae during nerve growth factor-induced differentiation. *J Biol Chem*. 2003;**278**:8706-16.

[78] Campenot RB, MacInnis BL. Retrograde transport of neurotrophins: fact and function. *J Neurobiol*. 2004;**58**:217-29.

[79] Cheng JK, Ji RR. Intracellular signaling in primary sensory neurons and persistent pain. *Neurochem Res*. 2008;**33**:1970-8.

[80] Zhu W, Oxford GS. Phosphoinositide-3-kinase and mitogen activated protein kinase signaling pathways mediate acute NGF sensitization of TRPV1. *Mol Cell Neurosci*. 2007;**34**:689-700.

[81] Wang H, Ehnert C, Brenner GJ, Woolf CJ. Bradykinin and peripheral sensitization. *Biol Chem*. 2006;**387**:11-4.

[82] Amaya F, Shimosato G, Nagano M, et al. NGF and GDNF differentially regulate TRPV1 expression that contributes to development of inflammatory thermal hyperalgesia. *Eur J Neurosci*. 2004;**20**:2303-10.

[83] Lindsay RM, Harmar AJ. Nerve growth factor regulates expression of neuropeptide genes in adult sensory neurons. *Nature*. 1989;**337**:362-4.

[84] Bonini S, Rasi G, Bracci-Laudiero ML, Procoli A, Aloe L. Nerve growth factor: neurotrophin or cytokine? *Int Arch Allergy Immunol*. 2003;**131**:80-4.

[85] De Benedetto A, Agnihothri R, McGirt LY, Bankova LG, Beck LA. Atopic dermatitis: a disease caused by innate immune defects? *J Invest Dermatol*. 2009;**129**:14-30.

[86] Lee MR, Cooper AJ. Immunopathogenesis of psoriasis. *Australas J Dermatol*. 2006;**47**:151-9.

[87] Bovenschen HJ, Seyger MM, Van de Kerkhof PC. Plaque psoriasis vs. atopic dermatitis and lichen planus: a comparison for lesional T-cell subsets, epidermal proliferation and differentiation. *Br J Dermatol*. 2005;**153**:72-8.

[88] Jiang WY, Raychaudhuri SP, Farber EM. Double-labeled immunofluorescence study of cutaneous nerves in psoriasis. *Int J Dermatol*. 1998;**37**:572-4.

[89] Jarvikallio A, Harvima IT, Naukkarinen A. Mast cells, nerves and neuropeptides in atopic dermatitis and nummular eczema. *Arch Dermatol Res*. 2003;**295**:2-7.

[90] Yamaguchi J, Aihara M, Kobayashi Y, Kambara T, Ikezawa Z. Quantitative analysis of nerve growth factor (NGF) in the atopic dermatitis and psoriasis horny layer and effect of treatment on NGF in atopic dermatitis. *J Dermatol Sci*. 2009;**53**:48-54.

[91] Kitamura T, Tange T, Terasawa T, et al. Establishment and characterization of a unique human cell line that proliferates dependently on GM-CSF, IL-3, or erythropoietin. *J Cell Physiol*. 1989;**140**:323-34.

[92] Balme E, Roth DR, Perentes E. Malignant spinal meningioma in a CD-1 mouse. *Exp Toxicol Pathol*. 2008;**60**:263-7.

[93]   Ronnov-Jessen L, Celis JE, Van Deurs B, Petersen OW. A fibroblast-associated antigen: characterization in fibroblasts and immunoreactivity in smooth muscle differentiated stromal cells. *J Histochem Cytochem.* 1992;**40**:475-86.

[94]   Ulmann L, Rodeau JL, Danoux L, Contet-Audonneau JL, Pauly G, Schlichter R. Trophic effects of keratinocytes on the axonal development of sensory neurons in a coculture model. *Eur J Neurosci.* 2007;**26**:113-25.

[95]   Schmidt LD, Xie Y, Lyte M, Vulchanova L, Brown DR. Autonomic neurotransmitters modulate immunoglobulin A secretion in porcine colonic mucosa. *J Neuroimmunol.* 2007;**185**:20-8.

[96]   Wong HC, Tache Y, Lloyd KC, et al. Monoclonal antibody to rat alpha-CGRP: production, characterization, and in vivo immunoneutralization activity. *Hybridoma.* 1993;**12**:93-106.

[97]   Drummond HA, Furtado MM, Myers S, et al. ENaC proteins are required for NGF-induced neurite growth. *Am J Physiol Cell Physiol.* 2006;**290**:C404-10.

[98]   Ioi H, Kido MA, Zhang JQ, et al. Capsaicin receptor expression in the rat temporomandibular joint. *Cell Tissue Res.* 2006;**325**:47-54.

[99]   Hingtgen CM, Roy SL, Clapp DW. Stimulus-evoked release of neuropeptides is enhanced in sensory neurons from mice with a heterozygous mutation of the Nf1 gene. *Neuroscience.* 2006;**137**:637-45.

[100]   Pincelli C, Sevignani C, Manfredini R, et al. Expression and function of nerve growth factor and nerve growth factor receptor on cultured keratinocytes. *J Invest Dermatol.* 1994;**103**:13-8.

[101]   Manni L, Lundeberg T, Fiorito S, Bonini S, Vigneti E, Aloe L. Nerve growth factor release by human synovial fibroblasts prior to and following exposure to tumor necrosis factor-alpha, interleukin-1 beta and cholecystokinin-8: the possible role of NGF in the inflammatory response. *Clin Exp Rheumatol.* 2003;**21**:617-24.

[102]   Hattori A, Hayashi K, Kohno M. Tumor necrosis factor (TNF) stimulates the production of nerve growth factor in fibroblasts via the 55-kDa type 1 TNF receptor. *FEBS Lett.* 1996;**379**:157-60.

[103]   Fernandez J, Nicholls JG. Fine structure and development of dorsal root ganglion neurons and Schwann cells in the newborn opossum Monodelphis domestica. *J Comp Neurol.* 1998;**396**:338-50.

[104]   Lin Q, Li D, Xu X, Zou X, Fang L. Roles of TRPV1 and neuropeptidergic receptors in dorsal root reflex-mediated neurogenic inflammation induced by intradermal injection of capsaicin. *Mol Pain.* 2007;**3**:30.

[105]   Munger BL, Ide C. The structure and function of cutaneous sensory receptors. *Arch Histol Cytol.* 1988;**51**:1-34.

[106]   Lind NM, Moustgaard A, Jelsing J, Vajta G, Cumming P, Hansen AK. The use of pigs in neuroscience: modeling brain disorders. *Neurosci Biobehav Rev.* 2007;**31**:728-51.

[107]   Rukwied R, Dusch M, Schley M, Forsch E, Schmelz M. Nociceptor sensitization to mechanical and thermal stimuli in pig skin in vivo. *Eur J Pain.* 2008;**12**:242-50.

[108]   Dou YC, Hagstromer L, Emtestam L, Johansson O. Increased nerve growth factor and its receptors in atopic dermatitis: an immunohistochemical study. *Arch Dermatol Res.* 2006;**298**:31-7.

[109]   Lewis T. The blood vessels of human skin and their responses. *London: Shaw and Sons.* 1927.

[110] Willis WD, Jr. Dorsal root potentials and dorsal root reflexes: a double-edged sword. *Exp Brain Res*. 1999;**124**:395-421.

[111] Chapman LF. Mechanisms of the flare reaction in human skin. *J Invest Dermatol*. 1977;**69**:88-97.

[112] Bayliss WM. On the origin from the spinal cord of the vaso-dilator fibres of the hind-limb, and on the nature of these fibres. *J Physiol*. 1901;**26**:173-209.

[113] Maggi CA, Meli A. The sensory-efferent function of capsaicin-sensitive sensory neurons. *Gen Pharmacol*. 1988;**19**:1-43.

[114] Beiswenger KK, Calcutt NA, Mizisin AP. Epidermal nerve fiber quantification in the assessment of diabetic neuropathy. *Acta Histochem*. 2008;**110**:351-62.

[115] Raychaudhuri SP, Jiang WY, Farber EM. Psoriatic keratinocytes express high levels of nerve growth factor. *Acta Derm Venereol*. 1998;**78**:84-6.

[116] Anand P, Terenghi G, Warner G, Kopelman P, Williams-Chestnut RE, Sinicropi DV. The role of endogenous nerve growth factor in human diabetic neuropathy. *Nat Med*. 1996;**2**:703-7.

[117] Blasing H, Hendrix S, Paus R. Pro-inflammatory cytokines upregulate the skin immunoreactivity for NGF, NT-3, NT-4 and their receptor, p75NTR in vivo: a preliminary report. *Arch Dermatol Res*. 2005;**296**:580-4.

[118] Saarma M. GDNF - a stranger in the TGF-beta superfamily? *Eur J Biochem*. 2000;**267**:6968-71.

[119] Zwick M, Davis BM, Woodbury CJ, et al. Glial cell line-derived neurotrophic factor is a survival factor for isolectin B4-positive, but not vanilloid receptor 1-positive, neurons in the mouse. *J Neurosci*. 2002;**22**:4057-65.

[120] Tokime K, Katoh-Semba R, Yamanaka K, Mizoguchi A, Mizutani H. Enhanced production and secretion of glial cell line-derived neurotrophic factor and nerve growth factor from the skin in atopic dermatitis mouse model. *Arch Dermatol Res*. 2008;**300**:343-52.

[121] Albers KM, Woodbury CJ, Ritter AM, Davis BM, Koerber HR. Glial cell-line-derived neurotrophic factor expression in skin alters the mechanical sensitivity of cutaneous nociceptors. *J Neurosci*. 2006;**26**:2981-90.

[122] Bogen O, Joseph EK, Chen X, Levine JD. GDNF hyperalgesia is mediated by PLCgamma, MAPK/ERK, PI3K, CDK5 and Src family kinase signaling and dependent on the IB4-binding protein versican. *Eur J Neurosci*. 2008;**28**:12-9.

9   Abbreviations

μg	Microgram
μL	Microliter
μm	Micrometer
AD	Atopic Dermatitis
BDNF	Brain-derived neurotrophic factor
CGRP	Calcitonin gene-related peptide
CNS	Central nervous system
CPNL	Cumulative peripheral neurite length
CPS	Capsaicin
CPZ	Capsazepine
CRLR	Calcitonin-receptor-like-receptor
CT	Calcitonin
DAPI	4',6-diamidino-2-phenylindole, dihydrochloride
DMEM	Dulbecco's Modified Eagle Medium
DRG	Dorsal root ganglia
EC_{50}	Half effective concentration
GDNF	Glial cell-derived neurotrophic factor
GFRa1-4	GDNF family receptor alpha 1-4
HDMECs	Human dermal microvascular endothelial cells
HEPES	4-(2-hydroxyethyl)-1-piperazineethanesulfonic acid
huNGFb	Recombinant human NGF
IB4	Isolectin B4
IL	Interleukin
m/s	meter per seconds
max.	Maximum
min	Minutes
mL	Milliliter
n	Number of independent data sets
NF200	Heavy neurofilament 200 kDa
ng	Nanogram
NGFb	Beta subunit of Nerve growth factor
NK	Neurokinin
NT-3	Neurotrophin-3
NT-4	Neurotrophin-4
PACAP	Pituitary adenylate cyclase activating protein
PBS	Phosphate buffered saline
PNS	Peripheral nervous system
POMC	Proopiomelanocortin
RAMP	Receptor-activity-modifying-protein
RT	Room temperature
SP	Substance P

|	
SST	Somatostatin
TG	Trigeminal ganglia
TNFa	Tumor necrosis factor alpha
TrkA	Receptor tyrosine kinase A
TRPV1	Transient receptor potential vanilloid 1
UV	Ultraviolet light
VIP	Vascular intestinal peptide

10 Index of Figures

11   Curriculum vitae

http://home.pages.at/susanne_falkner

Personal Details

Name:	Susanne Martina Falkner
Address:	Blindendorf 226
	4312 Ried / Riedmark
	Austria
Nationality:	Austria
Date of Birth:	15. March 1985 in Linz
Email:	s.falkner@gmx.at
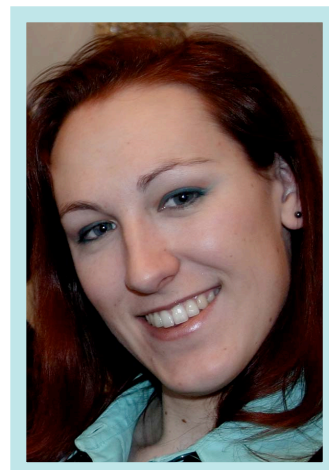
School education

February 2007	First Degree (equal to Bachelor) in Molecular Biology; Graduation with distinction
October 2003 – present	Studies in Molecular Biology at the University of Vienna, Campus Vienna BioCenter
1995 – 24.06.2003	Academic high school BRG Hamerling Linz; Graduation with distinction, grade 1.0
1991 – 1995	Elementary school in Linz, Kleinmünchen

Research experience

March – December 2008	Diploma thesis within a cooperational project between Beiersdorf AG, Hamburg and the University of Heidelberg; Groups of Dr. Gitta Neufang and Prof. Dr. Martin Schmelz, respectively; Field of thesis: Peripheral Nervous system *Neurotrophic Dependency of Sensory Neurons in a Co-Culture Model of Porcine DRGs and Human Skin Cells*
August – November 2007	Internship at Beiersdorf AG, Hamburg; Skin Research Department; Laboratory led by Dr. Gitta Neufang, supervisor Dr. Fatemeh Navid

July 2007	Practical course in Structural Biology at the Department of Biomolecular Structural Chemistry, University of Vienna, led by Prof.Dr. Konrat
March 2006 – July 2007	Working with supervisor Dr. Katarzina Lechward at the Institute of Medical Biochemistry; Abstracts concerning this work were presented at the Annual Mid-Term Meeting of the RTN Network „Flippases" in August 2006 in Copenhagen and at the 3rd Int. Forum on Oxidative Stress and Aging in Nagoya in September 2006
October 2005 – June 2007	Staff member of the Kuchler Laboratory at the Institute of Medical Biochemistry, Medical University of Vienna, led by Ao.Univ.Prof.Dr.Karl Kuchler
October – November 2006	Practical course in Neuroscience at the Brain Research Institute of Vienna led by Ao.Univ.Prof Johannes Berger
August 2006	Practical work in Biochemistry at the Institute of Biochemistry and Molecular Cell Biology, University of Vienna, laboratory of Ao.Univ.Prof.Dr. Gustav Ammerer
August – September 2005	Employment at the HLA-Laboratory at the Blood Center Linz, led by Prim.Dr.Christian Gabriel
January – March 2005	Human dissection practical course at the Institute of Anatomy, University of Vienna

Scholarships and awards

2005, 2006	Performance Scholarships awarded by the University of Vienna for outstanding achievements in Molecular Biology (in retrospect to passed courses and exams)

Language and additional skills

Languages	German, English, French
Certificates	FELASA category B; Permit for animal experiments